



**HAL**  
open science

# Design via topology optimisation and experimental assessment of thermal metadevices for conductive heat flux shielding in transient regime

Juan Carlos Álvarez-Hostos, Bruno Storti, Nicolas Lefevre, Vincent Sobotka, Steven Le Corre, Víctor Fachinotti

► **To cite this version:**

Juan Carlos Álvarez-Hostos, Bruno Storti, Nicolas Lefevre, Vincent Sobotka, Steven Le Corre, et al.. Design via topology optimisation and experimental assessment of thermal metadevices for conductive heat flux shielding in transient regime. *International Journal of Heat and Mass Transfer*, 2023, 212, pp.124238. 10.1016/j.ijheatmasstransfer.2023.124238 . hal-04111320

**HAL Id: hal-04111320**

**<https://hal.science/hal-04111320>**

Submitted on 5 Jun 2023

**HAL** is a multi-disciplinary open access archive for the deposit and dissemination of scientific research documents, whether they are published or not. The documents may come from teaching and research institutions in France or abroad, or from public or private research centers.

L'archive ouverte pluridisciplinaire **HAL**, est destinée au dépôt et à la diffusion de documents scientifiques de niveau recherche, publiés ou non, émanant des établissements d'enseignement et de recherche français ou étrangers, des laboratoires publics ou privés.

# Design via topology optimisation and experimental assessment of thermal metadevices for conductive heat flux shielding in transient regime

Juan C. Álvarez Hostos<sup>a,b</sup>, Bruno Storti<sup>c,d</sup>, Nicolas Lefevre<sup>c</sup>, Vincent Sobotka<sup>c</sup>, Steven Le Corre<sup>c</sup>, Víctor D. Fachinotti<sup>\*d</sup>

<sup>a</sup>Centro de Investigación y Transferencia (CIT) Rafaela, Universidad Nacional de Rafaela (UNRaf)/Consejo Nacional de Investigación Científicas y Técnicas (CONICET), Rafaela, Argentina

<sup>b</sup>Department of Materials, Faculty of Chemical Engineering, Universidad Nacional del Litoral (UNL), Santa Fe, Argentina.

<sup>c</sup>Université de Nantes, CNRS, Laboratoire de thermique et énergie de Nantes, LTeN, UMR 6607, Nantes F-44000, France.

<sup>d</sup>Centro de Investigación de Métodos Computacionales (CIMEC), Universidad Nacional del Litoral (UNL)/Consejo Nacional de Investigaciones Científicas y Técnicas (CONICET), Predio CCT-CONICET Santa Fe, Argentina.

## Abstract

The design via density-based topology optimisation (TO) of thermal metadevices for conductive heat flux manipulation in transient regime is introduced in this work. Such approach consists in the solution of a TO problem conceived to achieve simple devices of feasible manufacture, which are made of two macroscopically distinguishable isotropic materials of highly contrasting thermal properties. The objective function to be minimised during the solution of such TO problem is defined as the error in achieving a prescribed behaviour of the conductive heat flux in the region intended for its manipulation, and the well-known solid isotropic material with penalisation (SIMP) technique is used to define the material distribution as a continuous function. The finite element method is used for the numerical analysis of the metadevices performance, and for each finite element there is a single microparameter (artificial density) determining the material from which it is made. The proposed approach has been particularly applied to the design of metadevices to shield the conductive heat flux in a given region during a transient heat conduction process. Although the so-designed metadevices are made of standard isotropic materials, they actually behave as metamaterials allowing the desired manipulation of the heat flux. Such approach has been implemented in the design of an easy-to-manufacture metadvice capable of fulfilling the assigned task better than other design merely based on intuition, whose material distribution was conceived to at least roughly emulate the heterogeneous effective properties dictated by the method of transformation thermodynamics. Since the microparameters directly define the distribution of both isotropic materials, it has also been possible to manufacture a metadvice designed under the proposed approach and to experimentally evaluate its performance.

**Keywords:** Topology Optimisation, Metadevices, Heat flux manipulation, Shielding, Metamaterials, Sensitivity analysis

## 1. Introduction

Nowadays, the increasing development of metamaterials and metadevices (devices made of metamaterials or that macroscopically behave as such) allows the manipulation of several physical fields in extreme and unprecedented ways. Such an outstanding potential of both metamaterials and metadevices has found noteworthy applications in optics and electromagnetism<sup>[1]</sup>, sounds and vibrations<sup>[2,3]</sup>, heat transfer<sup>[4–21]</sup>, mass transfer<sup>[22–25]</sup>, mechanics<sup>[26–28]</sup> and thermo-mechanics<sup>[29–31]</sup>. Most of the metamaterials conceived for the aforementioned applications have been designed using the standard coordinates transformation approach originally introduced by Leonhardt<sup>[32]</sup> and Pendry<sup>[33]</sup> in the context of electromagnetism, whose particular implementation in the search for invariant forms of the heat conduction equation for several conductive heat flux manipulation purposes has given rise to the concept of transformation thermodynamics (TT)<sup>[18,34,35]</sup>. The TT approach has been widely and successfully implemented in the design of many thermal

metadevices for several conductive heat flux manipulation purposes, such as cloaking<sup>[4,5,12,15,36]</sup>, shielding<sup>[4,36]</sup>, concentrating<sup>[6,12,13,36]</sup> and reversing<sup>[12,36]</sup>.

Although the emergence of TT methods has given rise to novel possibilities of conductive heat flux manipulation through the design of metadevices for such purpose, this approach has also exhibited the following limitations concerning its feasibility and practical implementation:

- The heterogeneously distributed effective properties resulting from the TT procedure are not only anisotropic, but could also exhibit singular values (infinite and null thermal conductivity) at some positions of the regions intended for heat flux manipulation<sup>[4,8,13,18,36]</sup>.
- Since the TT method considers the regions of heat manipulation and heterogeneous material distribution to

---

\*Corresponding author: Fachinotti Víctor D. Currently main researcher at: Computational Methods Research Centre, National Scientific and Technical Research Council, Argentina. Contact email: vfachinotti@santafe-conicet.gov.ar

be defined after coordinate transformations, it usually involves very simple geometries and boundary conditions. The problems addressed via such technique are mostly defined over two-dimensional rectangular or circular geometries subjected to a homogeneous heat flux, whereas the metadevices encompass an annulus surrounding a circular region where the heat flux is manipulated [5,6,12,13,37].

- Any change in the problem geometry, heat flux manipulation task or boundary conditions introduces changes in the distribution of effective properties, whereby a different TT problem must be formulated and solved for each case [4,12,36–38].
- It provides information concerning the distribution of effective properties required to perform the heat flux manipulation task, but not about how to obtain such properties. This aspect of TT approaches leads to the need of searching for further ways to at least roughly emulate such effective properties, which is often achieved combining standard materials [4–6,15,37].

Several researchers have made special emphasis on proposing the design of feasible thermal metadevices capable of emulating the effective properties dictated by TT methods, mostly based on intuition [4–6,38]. On the other hand, Ji et al. [13] have recently introduced a more rigorous approach to emulate with standard materials the spatial distribution of the effective thermal conductivity tensor obtained from TT. Such procedure consists in considering a metadvice made of a composite material with a quantitatively characterisable microstructure, and finding at each position the required parameters in the microstructure so that the homogenised tensor of thermal conductivity corresponds to that obtained from TT. This technique has been particularly used in the design of conductive heat flux concentrators, and the so-designed devices exhibited a good performance. It is worth to mention the efforts made by some researchers to extend the TT methods to problems involving arbitrary geometries of both the metadvice and the region intended for heat flux manipulation [4,15,39,40], providing also in some cases interesting proposals concerning the combination of standard materials in order to emulate the distribution of effective properties dictated by the TT procedure [4,15]. After the pioneering work of Yang et al. [39] and Fu-Chun et al. [40] demonstrating the possibility of designing arbitrarily shaped shielding-cloaking metadevices via TT, Liu et al. [4] and Sha et al. [15] presented different approaches to manufacture TT-based thermal devices of non-conventional geometries. Liu et al. [4] relied on the possibility of approximating any geometry with polygons to use the TT approach in the design of N-sided polygonal thermal devices for simultaneous shielding and cloaking in transient regime, and demonstrated the possibility of achieving a good approximation of the effective properties distribution using a finite number of standard isotropic materials in bilayer configuration. Sha et al. [15] have recently introduced the implementation of 3-D printing technologies to man-

ufacture thermal metamaterials based on the assembling of small enough topological functional cells (TFCs), and the configuration of each TFC is such that the corresponding homogenised thermal conductivity tensor emulates that dictated by TT. As discussed so far, the main difficulties concerning the achievement of thermal metadevices based on TT are related to the need of emulate the distribution of highly anisotropic or even singular effective properties derived from the spatial transformations. Scattering cancellation (SC) is an alternative technique adopted by some researchers to avoid the often extreme effective properties inherent in TT [9,16–18], since the scattering method is independent of spatial transformations. Such procedure allows the design of thermal devices for conductive heat flux manipulation using only isotropic conductivities, since it is conceived via the analytical solution of the steady heat transfer equations of adjacent regions without introducing spatial transformations. These positive features have been properly used in the design of metadevices entirely based on natural isotropic bulk materials, such as: bilayer heat flux concentrators [9], rotating devices for adaptive thermal cloaking and shielding [16], interconnected structures for concentration and cloaking [18], and also monolayer thermal metadevices with switching functions between cloaking and invisibility [17]. There are still some noteworthy studies on alternative approaches to achieve feasible metadevices, such as the geometrically anisotropic heterogeneous composites for thermal invisibility developed by Tian et al. [14], and the recent developments on thermal carpet cloaks [8,41].

In addition to the widely known TT and SC methods, numerical optimisation is a technique that is becoming increasingly important in the design of thermal metamaterials [13,15] and metadevices [10,11,30,36,37,42–45]. Numerical optimisation has actually been used by Peralta et al. [42] to introduce a new paradigm in the design of thermal metadevices, which is the possibility of conceiving heat flux manipulation devices without a previous knowledge of the thermal property distributions dictated by TT or SC procedures. Given any metamaterial with a quantitatively characterisable microstructure, a large-scale continuous optimisation problem is formulated to directly determine the distribution of microparameters (parameters describing the microstructure) that minimises the error in the fulfilment of a heat flux manipulation task. This optimisation-based approach allows the direct prescription of how the metadvice is made, and the heterogeneous thermal properties are a direct consequence of the microparameters distribution obtained from the solution of the optimisation problem. The first metadvice designed by Peralta et al. [42] via such numerical optimisation-based approach consisted in a simultaneous heat concentration and cloaking device, which was conceived using a bilayered laminate metamaterial whose relative layer thickness and orientation were considered as the design variables to be optimised. Such a bilayered microstructure was subsequently used by Álvarez-Hostos et al. [30,37], who extended the approach proposed by Peralta et al. [42] to the design of thermo-mechanical cloaking [30]

and transient heat flux manipulation<sup>[37]</sup> metadevices. Although this optimisation-based metadevices design (OMD) approach directly dictates the metamaterial configuration at each point of the metadvice, achieving the particular heterogeneous distribution of microparameters resulting from the numerical optimisation procedure is actually an issue precluding the metadvice manufacture for real applications. In order to overcome the complexity of manufacturing such metadevices, Peralta et al.<sup>[43]</sup> proposed to use a finite number of candidate materials in the context of a discrete material optimisation technique, where the presence of each candidate material is dictated by an artificial density. In this sense, the work conducted by Peralta et al.<sup>[43]</sup> introduced the concept of topology optimisation-based metadevices design (TOMD). TOMD has made it possible to achieve feasible metadevices without resorting to heterogeneous distributions of anisotropic metamaterials, which was formerly considered a mandatory requirement for the extreme manipulation of macroscopic fields<sup>[13,15,42]</sup>. Fachinotti et al.<sup>[44]</sup> introduced a further development in TOMD by using the simple isotropic material with penalisation (SIMP) method in the design of an easy-to-make heat flux inversion metadvice consisting of two piecewise macroscopically distinguishable isotropic materials with contrasting thermal properties, which was also manufactured and successfully tested in a thermal experiment. Later, also Fachinotti et al.<sup>[28]</sup> successfully extended such idea to the design of easy-to-make elastostatic cloaking devices based on two piecewise macroscopically distinguishable isotropic materials with contrasting elastic properties. Subsequently, Álvarez-Hostos et al.<sup>[31]</sup> used the SIMP method in the TOMD approach in order to conceive easy-to-make thermo-mechanical cloaking devices. Such metadevices were designed allowing the dependence of elastic moduli with temperature, which was actually an unprecedented contribution to the design of thermo-mechanical metadevices. In addition to the aforementioned density-based topology optimisation approaches, several researchers are currently demonstrating the potential of level set-based TOMD for thermal cloaking and heat flux manipulation<sup>[7,10,11,19–21]</sup>. Fujii et al.<sup>[46]</sup> introduced the implementation of level-set-based TOMD for optical cloaking. After such a pioneer contribution, the potential of this procedure was demonstrated in the design of thermal carpet cloaks<sup>[7,10]</sup>, and metadevices for simultaneous heat flux concentration and thermal cloaking<sup>[11]</sup>. Xu et al.<sup>[21]</sup> introduced a further contribution in this field via the formulation of an extended level set method, which has consisted in extending the level set framework from an Euclidean to a Riemannian space to allow the free-form TOMD for thermal cloaking in a robust and remarkably simple manner. Such approach has been successfully implemented in the design of thermal cloaks in 2D, 3D shell and 3D solid domains, including also the cloaking of irregular inclusions. Nakagawa et al.<sup>[20]</sup> coupled the level set method to multiscale techniques in order to perform the TOMD for thermal cloaking and heat flux shielding, performing the level set-based topology optimisation of periodic microstructures in a finite number of predefined regions making up the metadvice. The mi-

crostructures of such regions are optimised in order to find a discrete macroscopic arrangement of homogenised thermal conductivities conceived to fulfil the tasks of thermal cloaking or heat flux shielding, or both simultaneously. The level set-based TOMD of thermal metadevices reported so far in the revised literature are devoted to steady state heat conduction problems. Luo et al.<sup>[19]</sup> performed the level set-based TOMD of steady state thermal cloaks using the lattice Boltzmann method for the heat conduction analysis, and also suggested the possibility of performing further work to extend such a novel procedure to transient heat conduction. The level set-based TOMD has the positive feature of suppressing “grey regions” (unfeasible materials with intermediate properties) without resorting to filtering techniques, whose implementation is mandatory in the framework of density-based procedures for the achievement of fully binary material distributions in the metadvice design<sup>[28,31,44]</sup>.

The aforementioned contributions concerning both OMD and TOMD approaches demonstrate the versatility and capabilities of these techniques in the design of metadevices, and the following positive features can be remarked:

- It is possible the design of metadevices based on any quantitatively characterised material, i.e. those materials whose effective properties are determined by particular microparameters.
- The design of metadevices in the context of problems involving any kind of geometry and boundary conditions is allowed.
- The distribution of microparameters (design variables) resulting from the solution of the optimisation problem directly dictates how the metadevices must be made, which is a crucial advantage with respect to those methods limited to only provide information concerning the distribution of heterogeneous and uncertainly feasible effective properties (like coordinates transformation-based approaches).
- It is not necessary to know the heterogeneous and often extreme effective properties previously dictated by TT or SC procedures, since such effective properties in OMD and TOMD approaches are a direct consequence of the distribution of microparameters characterising the metadvice microstructure at each point. The distribution of microparameters is determined via the solution of a unique continuous, non-linear, constrained, large-scale optimisation problem, which is remarkably more efficient than other procedures reported in the literature<sup>[13,15]</sup> where an optimisation problem must be solved at each point of the domain in order to find microparameters allowing the achievement of homogenised properties at least similar to those dictated by coordinates transformation-based techniques.
- Particularly in the case of TOMD approaches, these procedures allow the design of manufacturable and

high-performance metadevices based on a simple arrangement of a finite number of macroscopically distinguishable candidate materials [7,10,11,19–21,28,31,43,44].

It is worth to remark that neither density-based nor level set-based TOMD approaches have yet been used to achieve metadevices particularly conceived to perform conductive heat flux manipulation tasks in transient regime, whereby this communication is focused on demonstrating the relevance of accounting for transient effects in the design of thermal metadevices to be implemented under such conditions. The TOMD approach (and its advantages regarding manufacturability) is extended to the design of metadevices particularly devised to perform heat flux manipulation tasks in transient regime. The proposed procedure is particularly implemented in the design of heat flux shielding metadevices, which consisted in a very simple arrangement of two macroscopically distinguishable isotropic materials with contrasting thermal properties. A first metadvice is designed in order to compare its performance with respect to a TT-based metadvice built by Narayana et al. [47], since such communication is among the few work devoted to demonstrate the significance of considering transient heat conduction phenomena in the design of thermal metadevices. The results reported by Narayana et al. [47] demonstrated that the material distribution of metadevices devised to manipulate conductive heat flux in transient regime must be dictated not only in terms of an appropriate arrangement of the thermal conductivity, but also the volumetric heat capacity. Such aspects were subsequently considered by Álvarez Hostos et al. [37] in the microparameters-based OMD for transient heat flux shielding, using metamaterials of bilayered laminate microstructure. The metadvice designed by Álvarez Hostos et al. [37] exhibited a noteworthy superior performance with respect to the device devised by Narayana et al. [47], whereas the current work is devoted to achieve such outcomes using easy-to-make metadevices conceived via TOMD. Accordingly, the potential of this approach to achieve feasible manufacturing metadevices specifically designed to perform heat flux manipulation tasks in transient regime is first demonstrated by comparison with the results obtained by Narayana et al. [47]. The advantages regarding manufacturability of the proposed TOMD are used to design and manufacture a second shielding metadvice in a remarkably simple manner, using standard materials available to the authors in the *Laboratoire de Thermique et Énergie, Polytech, Nantes Université*. The metadvice is also numerically and experimentally tested, and the experimental results exhibit an excellent agreement with the performance predicted in the numerical simulations.

## 2. Governing equations

The OMD for thermal applications in transient regime involves the minimisation of a given objective function, which in this particular case is defined to quantify the error in accomplishing a prescribed heat flux manipulation task. The evaluation of such objective function requires to solve

the heat conduction equation in transient regime, which is performed in this work via the finite element method (FEM).

### 2.1. Transient heat conduction problem

The domain  $\Omega$  depicted in Fig. 1 represents a solid heterogeneous material undergoing a transient heat conduction process. The heat flux  $q_{\text{wall}}$  and temperature  $T_{\text{wall}}$  are prescribed on boundaries  $\Gamma_q$  and  $\Gamma_T$ , respectively. In transient regime, the temperature  $T$  in  $\Omega$  is governed by the following partial differential equation:

$$c \frac{\partial T}{\partial t} = \nabla \cdot (\mathbf{k} \nabla T) + \dot{q}, \quad (1)$$

where  $c$  is the volumetric heat capacity (density times the specific heat capacity),  $\mathbf{k}$  the thermal conductivity tensor and  $\dot{q}$  the internal heat source. The solution of (1) is subjected to the initial condition:

$$T = T_0 \quad \text{at } t = 0, \quad (2)$$

and the boundary conditions:

$$\begin{aligned} T &= T_{\text{wall}} & \text{on } \Gamma_T, \\ -\mathbf{k} \nabla T \cdot \mathbf{n} &= q_{\text{wall}} & \text{on } \Gamma_q, \end{aligned} \quad (3)$$

where  $\mathbf{n}$  is the normal unit vector pointing outwards  $\Gamma_q$ .

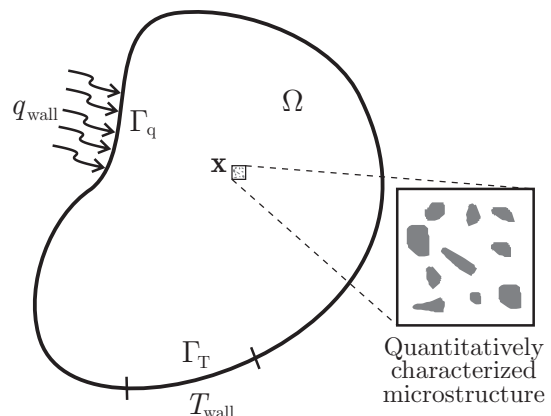


Figure 1: Transient heat conduction problem in a macroscopic heterogeneous domain with effective properties depending on a quantitatively characterised microstructure.

### 2.2. Finite element formulation

The transient heat conduction problem described in the previous section will be solved via the finite element method (FEM), which consists in using the following linear combination of basis functions to approximate the temperature field in the standard Bunov-Galerkin weak-form of the problem described by eq. (1)-(3):

$$T(\mathbf{x}) \approx N_i(\mathbf{x})T_i = \mathbf{N}(\mathbf{x})\mathbf{T}, \quad (4)$$

where  $T_i$  is the temperature unknown at each node  $\mathbf{x}_i$  of the finite element mesh, and  $N_i(\mathbf{x})$  is a standard interpolating shape function associated to this node such that  $N_i(\mathbf{x}_j) = \delta_{ij}$  with  $\delta_{ij}$  denoting the Kronecker delta [48]. Fulfilling the Kronecker delta property means that the value of the shape function of a given node is unit at its position ( $N_i(\mathbf{x}_i) = 1$ ) and null at the any other nodal position

( $N_i(\mathbf{x}_j) = 0$  for  $i \neq j$ ).  $T_i$  and  $N_i$  are grouped in vectors  $\mathbf{T}$  and  $\mathbf{N}$ , respectively. The substitution of eq. (4) in the Bunov-Galerkin weak-form of the transient heat conduction equations leads to the following semi-discrete problem for the vector of temperature unknowns<sup>[49]</sup>:

$$\mathbf{C}\dot{\mathbf{T}} + \mathbf{K}\mathbf{T} = \mathbf{Q}, \quad (5)$$

with

$$\begin{aligned} \mathbf{C} &= \int_{\Omega} \mathbf{N}^T c \mathbf{N} \, d\Omega, \\ \mathbf{K} &= \int_{\Omega} \mathbf{B}^T \mathbf{k} \mathbf{B} \, d\Omega, \\ \mathbf{Q} &= \underbrace{\int_{\Omega} \mathbf{N}^T \dot{q} \, d\Omega}_{\mathbf{Q}^i} - \underbrace{\int_{\Gamma_q} \mathbf{N}^T q^{\text{wall}} \, d\Gamma_q}_{\mathbf{Q}^q}, \end{aligned} \quad (6)$$

where  $\mathbf{B}$  is the matrix of components  $B_{ij} = \partial N_i / \partial x_j$  such that  $\nabla T \approx \mathbf{B}\mathbf{T}$ . The transient term of the semi-discrete problem (5) is numerically integrated under a fully implicit backward difference scheme, which leads to an algebraic system of equations for the vector of temperature unknowns at time  $n\Delta t$ :

$$\mathbf{C} \frac{\mathbf{T}^{n\Delta t} - \mathbf{T}^{(n-1)\Delta t}}{\Delta t} + \mathbf{K}\mathbf{T}^{n\Delta t} = \mathbf{Q}^{n\Delta t}, \quad (7)$$

where  $n$  is an integer between 1 and  $N_t$ , and  $N_t$  is the number of time steps used in the time integration. Eq. (7) is solved once the previous vector of temperature  $\mathbf{T}^{(n-1)\Delta t}$  is known.

### 2.3. TOMD for transient heat flux manipulation

Let a metadvice occupy a non-homogeneous region  $\Omega_{\text{dev}} \subset \Omega$  such that the microstructure at each finite element  $\Omega_e$  is quantitatively characterised (as depicted in Fig.1), so that both the effective volumetric heat capacity and effective tensor of thermal conductivity at  $\Omega_e$  are defined by a set of  $M$  microparameters grouped in the vector of design variables  $\mathbf{p}_e$ . Examples of microparameters defining the properties of a quantitatively characterisable microstructure are the geometrical parameters defining a biomimetic unit cell of artificial bones<sup>[50,51]</sup>, the relative thickness of layers and their orientation in laminates<sup>[30,37,42]</sup>, the orientation of nonspherical inclusions in composites<sup>[52]</sup>, among others. The density-based TOMD can be interpreted as a particular case of the microparameters-based OMD where the design variables are no longer microparameters defining the properties of a quantitatively characterisable microstructure, but artificial densities defining the macroscopic distribution of a finite number of candidate materials<sup>[28,31,43,44]</sup>. In agreement with the aspects discussed so far, the global capacitance  $\mathbf{C}$  and conduction  $\mathbf{K}$  matrices are such that:

$$\mathbf{C} = \mathbf{C}(\mathbf{P}), \quad \mathbf{K} = \mathbf{K}(\mathbf{P}), \quad (8)$$

with

$$\mathbf{P} = [\mathbf{p}_1, \mathbf{p}_2, \dots, \mathbf{p}_N], \quad (9)$$

whereby the transient temperature distribution in the whole domain  $\Omega$  depends on  $\mathbf{P}$ , i.e.  $T = T(\mathbf{x}, t, \mathbf{P})$  for all  $\mathbf{x} \in \Omega$ <sup>[37]</sup>.

According to the Fourier's Law, the conductive heat flux  $\mathbf{q}$  in a continuous medium is given by:

$$\mathbf{q} = -\mathbf{k}\nabla T. \quad (10)$$

For each finite element  $\Omega_e$ , the heat flux at a given point  $\mathbf{x}$  inside the element is:

$$\mathbf{q}_e(\mathbf{x}, t) = -\mathbf{k}_e \mathbf{B}_e(\mathbf{x}) \mathbf{T}_e(\mathbf{P}, t) = \mathbf{q}_e(\mathbf{P}, \mathbf{x}, t), \quad (11)$$

where  $\mathbf{k}_e$  is the thermal conductivity at the finite element  $\Omega_e$ , being  $\mathbf{k}_e = \mathbf{k}(\mathbf{p}_e)$  for  $\Omega_e \in \Omega_{\text{dev}}$  and fixed otherwise. The vector of unknown temperatures  $\mathbf{T}_e$  and the matrix of shape function gradients  $\mathbf{B}_e$  are restricted to the nodes used to interpolate the temperature field in  $\Omega_e$ .

The TOMD for transient heat flux manipulation consists in finding a distribution of microparameters  $\mathbf{P}$  such that the resulting microstructure throughout  $\Omega_{\text{dev}}$  allows the achievement of a prescribed behaviour of the heat flux in a region  $\Omega_{\text{task}} \in \Omega$ , i.e. to find  $\mathbf{P}$  such that:

$$\mathbf{q}(\mathbf{P}, \mathbf{x}, t) = \bar{\mathbf{q}}(\mathbf{x}, t), \quad \text{for all } \mathbf{x} \in \Omega_{\text{task}}, \text{ and } t \in (0, t_f) \quad (12)$$

where  $\bar{\mathbf{q}}(\mathbf{x}, t)$  is the heat flux that must be achieved in the region  $\Omega_{\text{task}} \subset \Omega$  within the time interval  $(0, t_f)$ , according to the distribution of microparameters  $\mathbf{P}$  in the region  $\Omega_{\text{dev}} \subset \Omega$ . The TOMD versatility for the achievement of thermal cloaking and different heat flux manipulation tasks has already been demonstrated in the framework of both density-based<sup>[36,43,44]</sup> and level set-based<sup>[7,10,11,19-21]</sup> procedures, and the task to be fulfilled is set according to  $\bar{\mathbf{q}}(\mathbf{x}, t)$ . Such a prescribed heat flux can be defined in terms of a reference value  $\mathbf{q}_{\text{hom}}(\mathbf{x}, t)$  corresponding to the heat conduction in an homogeneous plate entirely made of the background material comprising  $\Omega_{\text{out}}$ , i.e.  $\bar{\mathbf{q}}(\mathbf{x}, t) = \gamma \mathbf{q}_{\text{hom}}(\mathbf{x}, t)$  ( $\gamma$  is a constant). Some examples include: **(i) Heat flux shielding**<sup>[20,37,44]</sup>:  $\gamma = 0$  in  $\Omega_{\text{shield}} \equiv \Omega_{\text{task}} = \Omega_{\text{in}}$ , **(ii) Heat flux concentration**<sup>[11,42-44]</sup>:  $\gamma > 1$  in  $\Omega_{\text{conc}} \equiv \Omega_{\text{task}} = \Omega_{\text{in}}$ , **(iii) Heat flux inversion**<sup>[37,44]</sup>:  $\gamma = -1$  in  $\Omega_{\text{inv}} \equiv \Omega_{\text{task}} = \Omega_{\text{in}}$ , and **(iv) Thermal cloaking of an inclusion**<sup>[7,10,19,21]</sup>:  $\gamma = 1$  in  $\Omega_{\text{cloak}} \equiv \Omega_{\text{task}} = \Omega_{\text{out}}$ . The microstructure feasibility is allowed constraining the search for  $\mathbf{P}$  to a feasible design set  $\mathcal{D}$ , which precludes the perfect fulfilment of the transient heat flux manipulation task. Therefore, the task fulfilment is accomplished up to a minimum error given by<sup>[37]</sup>:

$$f(\mathbf{P}) = \frac{1}{t_f} \int_0^{t_f} g(\mathbf{P}, t) dt / f_0 \quad \text{with} \quad f_0 = \frac{1}{t_f} \int_0^{t_f} g_0(t) dt, \quad (13)$$

where  $g$  is defined as the following root mean square error in fulfilling the task in  $\Omega_{\text{task}}$  at a given time  $t$ :

$$g(\mathbf{P}, t) = \left[ \frac{1}{\Omega_{\text{task}}} \int_{\Omega_{\text{task}}} \|\mathbf{q}(\mathbf{P}, \mathbf{x}, t) - \bar{\mathbf{q}}(\mathbf{x}, t)\|^2 \, d\Omega \right]^{1/2}, \quad (14)$$

and  $g_0$  is the root mean square error inherent in the heat flux field  $\mathbf{q}_0(\mathbf{x}, t)$  in the absence of metadvice:

$$g_0(t) = \left[ \frac{1}{\Omega_{\text{task}}} \int_{\Omega_{\text{task}}} \|\mathbf{q}_0(\mathbf{x}, t) - \bar{\mathbf{q}}(\mathbf{x}, t)\|^2 \, d\Omega \right]^{1/2}. \quad (15)$$

As performed in previous communications concerning both microparameters-based OMD<sup>[30,37,42]</sup> and density-based TOMD<sup>[28,31,43,44]</sup>, the accomplishment of the task defined in (14) is assessed in a discrete form at  $H$  finite number of points  $\mathbf{x}_h \in \Omega_{\text{task}}$  lying at the centre of each element  $\Delta\Omega_h \in \Omega_{\text{task}}$ :

$$g(\mathbf{P}, t) = \left[ \frac{1}{\sum_{h=1}^H \Delta\Omega_h} \sum_{h=1}^H \|\mathbf{q}(\mathbf{P}, \mathbf{x}_h, t) - \bar{\mathbf{q}}(\mathbf{x}_h, t)\|^2 \Delta\Omega_h \right]^{1/2}, \quad (16)$$

and  $g_0(t)$  is consistently computed as:

$$g_0(t) = \left[ \frac{1}{\sum_{h=1}^H \Delta\Omega_h} \sum_{h=1}^H \|\mathbf{q}_0(\mathbf{P}, \mathbf{x}_h, t) - \bar{\mathbf{q}}(\mathbf{x}_h, t)\|^2 \Delta\Omega_h \right]^{1/2}, \quad (17)$$

The FEM-based solutions will be performed over uniform meshes, for which  $\Delta\Omega_h / \sum_{h=1}^H \Delta\Omega_h = 1/H$ . The TOMD for heat flux manipulation in transient regime is performed solving the following non-linear constrained optimisation problem to minimise the error defined in (13):

$$\min_{\mathbf{P} \in \mathcal{D}} f(\mathbf{P}), \quad (18)$$

whereby the function  $f$  defining the error in fulfilling the transient heat flux manipulation task is actually the objective function to be minimised, and the microparameters  $\mathbf{p}_e$  defining the microstructure of each element  $\Omega_e \in \Omega_{\text{dev}}$  are the design variables. Such features lead to a large-scale optimisation problem, since there are  $M$  design variables (microparameters) per finite element  $\Omega_e \in \Omega_{\text{dev}}$ .

A microparameters-based OMD has been successfully performed in a previous communication<sup>[37]</sup> for transient heat flux manipulation, where the metadvice design was based on a metamaterial consisting in an orthotropic composite laminate made of two materials with highly contrasting thermal properties. Although it was demonstrated that such metadvice allows an excellent fulfilment of the heat flux manipulation task, the particular heterogeneous distribution of relative thickness and orientation of the bilayered laminate metamaterial from which it is made still precludes its manufacture for real applications. The introduction of manufacturability constraints has already been recognised to be crucial for the manufacture of thermal<sup>[7,11,19,21,43,44]</sup>, mechanical<sup>[28]</sup> and also thermo-mechanical<sup>[31]</sup> metadvice, whereby the current transient heat flux manipulation metadvice will be conceived under the TOMD approach in order to allow its manufacture. This feature will be assured via the implementation of a density-based SIMP approach, which has already been successfully used in TOMD procedures for thermal<sup>[44]</sup> and thermo-mechanical<sup>[31]</sup> applications. The thermal metadvice designed so far via TOMD techniques performed via both density-based<sup>[43,44]</sup> and level set-based<sup>[7,10,11,19–21]</sup> procedures have been limited to the fulfilment of heat flux manipulation tasks in steady regime, and this is actually the first work focused on properly extending the favourable features of such approach to the design of thermal metadvice in the context of transient heat conduction problems. Following the SIMP technique, the volumetric heat capacity and thermal conductivity are computed at each finite element

$\Omega_e \in \Omega_{\text{dev}}$  as follows:

$$\begin{aligned} c_e &= c_A + (c_B - c_A) \chi_e^p, \\ k_e &= k_A + (k_B - k_A) \chi_e^p, \end{aligned} \quad (19)$$

where  $p > 1$  is a penalty coefficient,  $\chi_e$  is an artificial density with  $0 \leq \chi_e \leq 1$ , whereas subscripts A and B represent two different isotropic materials. A value of  $p \geq 3$  is high enough to penalise  $\chi_e^p$  in order to make it tend to 0 or 1. It is worth to note that performing a TOMD under the SIMP technique introduces a single design variable  $\chi_e$  at each finite element  $\Omega_e \in \Omega_{\text{dev}}$ .  $\mathbf{p}_e$  is no longer a vector, but a scalar  $p_e = \chi_e$  ( $M = 1$ ) determining the isotropic material (A or B) occupying the element.

## 2.4. Sensitivity analysis

Since the transient term of the heat conduction problem is numerically integrated under a fully implicit backward difference scheme, the solution of the optimisation problem (18) will be performed assessing the objective function (13) in a discrete manner, i.e.:

$$f(\mathbf{P}) = \frac{1}{f_0 N_t} \sum_{n=1}^{N_t} g(\mathbf{P}, n\Delta t), \quad \text{with} \quad f_0 = \frac{1}{N_t} \sum_{n=1}^{N_t} g_0(n\Delta t). \quad (20)$$

The analytical computation of the sensitivity  $df/dP_i$  is crucial to perform an efficient solution of the optimisation problem (18), which in this work will be achieved using the adjoint method. For this purpose, an augmented form of the objective function is introduced following the work of Michaleris et al.<sup>[53]</sup>:

$$f(\mathbf{P}) = \frac{1}{N_t} \sum_{n=1}^{N_t} \left\{ \underbrace{g(\mathbf{P}, n\Delta t)}_{g^{n\Delta t}} - \left[ \boldsymbol{\lambda}^{n\Delta t} \right]^T \underbrace{\mathbf{R}(\mathbf{T}^{n\Delta t}, \mathbf{T}^{(n-1)\Delta t})}_{\mathbf{R}^{n\Delta t}} \right\}, \quad (21)$$

where:

$$\mathbf{R}^{n\Delta t} = \mathbf{C} \frac{\mathbf{T}^{n\Delta t} - \mathbf{T}^{(n-1)\Delta t}}{\Delta t} + \mathbf{K} \mathbf{T}^{n\Delta t} - \mathbf{Q}^{n\Delta t} = \mathbf{0} \quad (22)$$

is the residual form of the discretised heat balance equation (7).

The derivative of (21) with respect to the  $i$ -th component of  $\mathbf{P}$  is given by:

$$\begin{aligned} \frac{df}{dP_i} &= \frac{1}{N_t} \sum_{n=1}^{N_t} \left( \frac{\partial g^{n\Delta t}}{\partial P_i} + \frac{\partial g^{n\Delta t}}{\partial \mathbf{T}^{n\Delta t}} \frac{d\mathbf{T}^{n\Delta t}}{dP_i} \right) \\ &\quad - \frac{1}{N_t} \sum_{n=1}^{N_t} \left[ \boldsymbol{\lambda}^{n\Delta t} \right]^T \frac{\partial \mathbf{R}^{n\Delta t}}{\partial P_i} \\ &\quad - \frac{1}{N_t} \sum_{n=1}^{N_t} \left[ \boldsymbol{\lambda}^{n\Delta t} \right]^T \left( \frac{\partial \mathbf{R}^{n\Delta t}}{\partial \mathbf{T}^{n\Delta t}} \frac{d\mathbf{T}^{n\Delta t}}{dP_i} + \frac{\partial \mathbf{R}^{n\Delta t}}{\partial \mathbf{T}^{(n-1)\Delta t}} \frac{d\mathbf{T}^{(n-1)\Delta t}}{dP_i} \right), \end{aligned} \quad (23)$$

where:

$$\begin{aligned} \frac{\partial \mathbf{R}^{n\Delta t}}{\partial \mathbf{T}^{n\Delta t}} &= \frac{\mathbf{C}}{\Delta t} + \mathbf{K}, \\ \frac{\partial \mathbf{R}^{n\Delta t}}{\partial \mathbf{T}^{(n-1)\Delta t}} &= -\frac{\mathbf{C}}{\Delta t}, \end{aligned} \quad (24)$$

whereas:

$$\frac{\partial \mathbf{R}^{n\Delta t}}{\partial P_i} = \frac{d\mathbf{C}}{dP_i} \frac{\mathbf{T}^{n\Delta t} - \mathbf{T}^{(n-1)\Delta t}}{\Delta t} + \frac{d\mathbf{K}}{dP_i} \mathbf{T}^{n\Delta t} - \frac{d\mathbf{Q}^{n\Delta t}}{dP_i} \quad (25)$$

The adjoint vectors  $\boldsymbol{\lambda}^{n\Delta t}$  must be determined in order to avoid the expensive computation of  $d\mathbf{T}^{n\Delta t}/dP_i$  and  $d\mathbf{T}^{(n-1)\Delta t}/dP_i$ , which are consequently obtained from the solution of the following set of adjoint problems:

$$\begin{aligned} \left[ \frac{\partial \mathbf{R}^{N_t \Delta t}}{\partial \mathbf{T}^{N_t \Delta t}} \right]^T \boldsymbol{\lambda}^{N_t \Delta t} &= \left[ \frac{\partial g^{N_t \Delta t}}{\partial \mathbf{T}^{N_t \Delta t}} \right]^T, \\ \left[ \frac{\partial \mathbf{R}^{(n-1)\Delta t}}{\partial \mathbf{T}^{(n-1)\Delta t}} \right]^T \boldsymbol{\lambda}^{(n-1)\Delta t} &= \left[ \frac{\partial g^{(n-1)\Delta t}}{\partial \mathbf{T}^{(n-1)\Delta t}} \right]^T - \left[ \frac{\partial \mathbf{R}^{n\Delta t}}{\partial \mathbf{T}^{(n-1)\Delta t}} \right]^T \boldsymbol{\lambda}^{n\Delta t}. \end{aligned} \quad (26)$$

The set of adjoint problems must be solved for  $n = N_t, N_t - 1, N_t - 2, \dots, 1$  (in this order), and the objective function sensitivity with the design variables is subsequently computed from:

$$\frac{df}{dP_i} = \frac{1}{N_t} \sum_{n=1}^{N_t} \left( \frac{\partial g^{n\Delta t}}{\partial P_i} - [\boldsymbol{\lambda}^{n\Delta t}]^T \frac{\partial \mathbf{R}^{n\Delta t}}{\partial P_i} \right), \quad (27)$$

### 3. Design of a metadvice for transient heat flux manipulation

The current section presents an example of application of TOMD for heat flux manipulation in transient regime, particularly for heat flux shielding. The performance of a first metadvice designed using such approach will be compared to that of a metadvice proposed by Narayana et al.<sup>[47]</sup> for the same purpose, whose material distribution was conceived to at least roughly emulate the thermal properties dictated by TT. In this sense, the current TOMD will be performed in the context of a heat transfer problem assuming the geometry, material properties and boundary conditions considered in the work of Narayana et al.<sup>[47]</sup>. Subsequently, a second shielding metadvice also designed via TOMD but using the materials available at the laboratory will be manufactured and its performance will be experimentally tested. The domain  $\Omega = \Omega_{\text{out}} \cup \Omega_{\text{in}} \cup \Omega_{\text{dev}}$  and boundary conditions of the transient heat conduction problem concerning the design of the heat flux shielding metadvice are depicted in Fig. 2, where  $\Omega_{\text{shield}} \equiv \Omega_{\text{task}} = \Omega_{\text{in}}$  is the region to be shielded. The shielding metadvice is designed to occupy the annular region  $\Omega_{\text{dev}}$  of inner and outer radii  $r$  and  $R$ , respectively. The domain is initially at a uniform temperature  $T_0$ , and the symmetry of both geometry and boundary conditions with respect to the  $x$ -axis allows the FEM-based solution of the problem meshing only the upper half of  $\Omega$ . The right boundary is kept at a temperature  $T_R$ , whereas the left boundary temperature is kept at  $T_L$  until a first steady state is reached at  $t = t_1$ , and it is subsequently increased to  $T_L^* = T_L + \Delta T_L$ . The transient analysis is finished at time  $t = t_f$ , when a new steady regime is reached. A metadvice made of two isotropic and macroscopically distinguishable candidate materials A and B occupying the annular region  $\Omega_{\text{dev}}$  is designed to make

the heat flux attain the prescribed value  $\bar{\mathbf{q}}(\mathbf{x}_h, t)$  at all the centres  $\mathbf{x}_h$  of the elements  $\Omega_e \in \Omega_{\text{task}}$ , which for shielding purposes ( $\Omega_{\text{task}} \equiv \Omega_{\text{shield}} = \Omega_{\text{in}}$ ) is set to be  $\bar{\mathbf{q}}(\mathbf{x}_h, t) = \mathbf{0}$ .

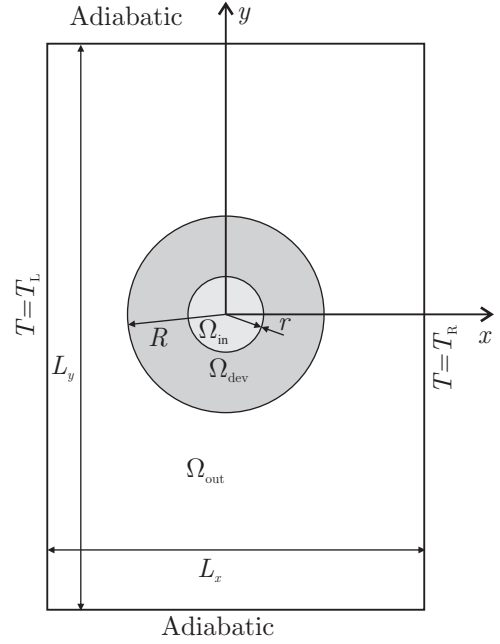


Figure 2: Domain  $\Omega = \Omega_{\text{out}} \cup \Omega_{\text{in}} \cup \Omega_{\text{dev}}$  and boundary conditions of the transient heat conduction problem concerning the TOMD for heat flux manipulation.

The continuous optimisation problem inherent in the TOMD procedure is solved in this work using the method of moving asymptotes (MMA)<sup>[54]</sup>, and the checkerboard patterns usually affecting the material distribution in topology optimisation problems<sup>[55]</sup> are eliminated via the Bruns and Tortorelli's<sup>[56]</sup> density filtering technique. The "grey" zones (those elements where  $0 < \chi_e < 1$ , i.e. made of an unfeasible material with intermediate properties between A and B) that remain despite the penalty coefficient  $p$  inherent in the SIMP method are significantly reduced using the Heaviside filtering proposed by Guest et al.<sup>[57]</sup>, which is implemented in the framework of a continuation approach proposed by Sigmund et al.<sup>[58,59]</sup>. Although this procedure leads to a noteworthy reduction of the grey zones, a further threshold filtering strategy successfully used in previous work concerning TOMD<sup>[28,31,44]</sup> is also implemented in order to obtain a fully binary material distribution in the metadvice. Although a comprehensive and detailed explanation concerning the filtering procedures mentioned above can be found in a previous communication<sup>[31]</sup>, it will be also described in this work. Coupling the density and Heaviside filtering techniques implies the computation of a filtered artificial density given by:

$$\tilde{P}_e = 1 - e^{-\beta \bar{P}_e} + \bar{P}_e e^{-\beta} \equiv \tilde{H}(\bar{P}_e, \beta), \quad (28)$$

with

$$\bar{P}_e = \frac{\sum_{i=1}^N \langle r - \Delta_{ei} \rangle P_i}{\sum_{i=1}^N \langle r - \Delta_{ei} \rangle}. \quad (29)$$

Eq.(29) defines the density filter<sup>[60]</sup>, where the filter radius  $r$  has been adopted in this work to be 7 times the finite

element size.  $\Delta_{ei}$  is the distance between the centres of elements  $\Omega_e$  and  $\Omega_i$ , whereas  $\langle \xi \rangle = \xi H(\xi)$  is the ramp function with  $H(\xi)$  denoting the Heaviside step function ( $H(\xi) = 0$  for  $\xi < 0$ ,  $H(0) = 1/2$  and  $H(\xi) = 1$  for  $\xi > 0$ ). In the Heaviside projection filtering<sup>[57]</sup> defined by Eq.(28)  $\tilde{H}(\xi, \beta)$  is a regularisation of  $H(\xi)$ , where the parameter  $\beta$  is such that  $\tilde{H}(\xi, 0) = \xi$  and  $\tilde{H}(\xi, \infty) = H(\xi)$ . The material properties at element  $\Omega_e$  are determined according to the value of  $\tilde{\chi}_e$ , whereby it is also called ‘‘physical’’ density<sup>[31]</sup>. Consequently, the objective function becomes  $\tilde{f}(\mathbf{P}) \equiv f(\tilde{\mathbf{P}})$  with  $\tilde{\mathbf{P}} = [\tilde{P}_1, \tilde{P}_2, \dots, \tilde{P}_N] = [\tilde{\chi}_1, \tilde{\chi}_2, \dots, \tilde{\chi}_N]$ , but  $\mathbf{P}$  still remains as design variable. Accordingly, the optimisation problem (18) is finally defined as

$$\min_{\mathbf{P} \in \mathcal{D}} \tilde{f}(\mathbf{P}), \quad \text{subjected to } 0 \leq P_i \leq 1 \quad i = 1, 2, \dots, N. \quad (30)$$

Due to filtering, Eq.(27) now actually defines  $d\tilde{f}/d\tilde{P}_i$  instead of  $df/dP_i$ . Such filtering must be considered during the sensitivity analysis, which is performed using the chain rule to compute the derivative of the new objective function with respect to the design variable  $P_i$ :

$$\frac{d\tilde{f}}{dP_i} = \frac{d\tilde{f}}{d\tilde{P}_j} \frac{d\tilde{P}_j}{dP_k} \frac{d\tilde{P}_k}{dP_i}, \quad (31)$$

where  $\frac{d\tilde{P}_j}{dP_k}$  and  $\frac{d\tilde{P}_k}{dP_i}$  can be easily obtained by derivation of Eqs.(28) and (29), respectively. The final design is achieved via the solution of successive optimisation problems, where the regularisation parameter  $\beta$  is gradually increased following the continuation approach<sup>[58,59]</sup>. This procedure is conceived to achieve stable convergence and ensuring differentiability in density-based topology optimisation procedures<sup>[58,59]</sup>, and its implementation is schematised in the following flowchart in pseudo code:

1. Initialisation: set  $s = 0$  and  $\mathbf{P}_0 = [0.5, 0.5, \dots, 0.5]$ .
2. Continuation: set  $\beta = 2^s$ ,  $i = 0$  and  $\mathbf{P}^{(i)} = \mathbf{P}_0$ .
  - (a) Transient heat conduction FEM:  $\tilde{\mathbf{P}} \rightarrow T(\mathbf{x}, t, \tilde{\mathbf{P}})$
  - (b) Objective function:  $T(\mathbf{x}, t, \tilde{\mathbf{P}}) \rightarrow f(\tilde{\mathbf{P}})$
  - (c) Sensitivity:  $(\mathbf{P}^{(i)}, \tilde{\mathbf{P}}, T, \dots) \rightarrow \partial f / \partial \mathbf{P}$
  - (d) Update:  $(\mathbf{P}^{(i)}, \partial f / \partial \mathbf{P}) \rightarrow \mathbf{P}^{(i+1)}$
  - (e) Stop criterion:
    - if  $i < i_{max}$  and  $\left\| \mathbf{P}^{(i+1)} - \mathbf{P}^{(i)} \right\|_{\infty} > \epsilon$ ,  $i \leftarrow i + 1$ , go to (a).
    - Otherwise:
      - if  $\beta < \beta_{max}$ , set  $s \leftarrow s + 1$  and  $\mathbf{P}_0 = \mathbf{P}^{(i+1)}$ , then go to (2).
      - Otherwise, go to (3).
3. Threshold filtering:  $(\tilde{\mathbf{P}}, w^*) \rightarrow \tilde{\mathbf{P}}^{thr}$

The initial guess of  $\mathbf{P}_0$  within the continuation procedure is arbitrarily adopted for  $\beta = 0$  (without Heaviside projection filtering), and then updated for each continuation step  $s$ . The optimisation solver stops at each continuation step when  $i = i_{max} = 150$  or the change in design variables is less than  $\epsilon = 0.01$ . The regularisation parameter of the Heaviside approximation is increased up to  $\beta_{max} = 128$  ( $s = 7$ ), for which the grey zones are significantly reduced<sup>[31]</sup>. Although the continuation approach allows the virtual elimination of unfeasible materials with intermediate properties

after the successive optimisation steps, a final filter (the so-called threshold filtering procedure) is still required to obtain a fully discrete (binary) material distribution  $\mathbf{P}^{thr}(w^*)$  with  $w^*$  as the threshold for  $\chi_e^p$ . Such a final filtering technique was proposed by Fachinotti et al.<sup>[44]</sup>, and successfully implemented in the TOMD for thermal<sup>[44]</sup>, mechanical<sup>[28]</sup> and thermo-mechanical<sup>[31]</sup> applications. The threshold filtering procedure consists in setting a threshold filtered density  $\tilde{P}_e^{thr}$  at each element  $\Omega_e \in \Omega_{dev}$  such that it is entirely made of material A ( $\tilde{P}_e^{thr} = 0$ ) or B ( $\tilde{P}_e^{thr} = 1$ ), with

$$\tilde{P}_e^{thr} = H(\tilde{P}_e - w^*) \quad (32)$$

where  $w^*$  is the threshold. In classical topology optimisation,  $w^*$  is a user-defined parameter often determined to fulfil volume constraints<sup>[61,62]</sup>. The threshold filtering strategy proposed by Fachinotti et al.<sup>[28,44]</sup> is particularly formulated for problems without volume constraints, such as the TOMD to be performed in this communication. The procedure consists of finding  $w^*$  for which the resulting discrete metadvice exhibits the best possible performance, in comparison with the still unfeasible material distribution with very narrow grey zones (that achieved for  $\beta = 128$ ). In short, such a final filtering procedure is performed to find  $w^* \in (0, 1)$  such that  $f^{thr}/f = f(\tilde{\mathbf{P}}^{thr})/f(\tilde{\mathbf{P}})$  reaches its minimum.

## 4. Numerical results and experimental validation

At a first stage, the TOMD procedure has been used to design a heat flux shielding metadvice with the geometry, material properties and boundary conditions of the problem addressed by Narayana et al.<sup>[47]</sup>. This first example has been included in order to compare the performance of an easy-to-manufacture metadvice achieved via TOMD to that exhibited by the design proposed by Narayana et al.<sup>[47]</sup>, which was based on TT and intuition. The proposed approach has been subsequently implemented in the design of a heat flux shielding metadvice to be manufactured with isotropic materials available to authors in the laboratory, which has also been tested experimentally in order to validate the shielding capabilities previously predicted via numerical analysis.

### 4.1. Comparison with a metadvice based on transformation thermodynamics and intuition

The plate geometry in the context of Narayana et al.<sup>[47]</sup> model is  $L_x = 0.1$  m wide and  $L_y = 0.15$  m height, and  $\Omega_{shield}$  has a radius of  $r = 0.01$  m. The inner and outer radii of the metadvice are  $r = 0.01$  m and  $R = 0.026$  m, respectively. For the TOMD procedure, the FEM-based solution of the governing equations has been performed discretising the upper half of the plate with a uniform mesh of  $200 \times 150 = 30000$  bilinear finite elements. Among all finite elements, 3614 have their centres within  $\Omega_{dev}$ . Since

the artificial density is considered to vary element-wise in  $\Omega_{\text{dev}}$ , the resulting non-linear large-scale constrained optimisation problem involves 3614 design variables. The domain regions  $\Omega_{\text{out}}$  and  $\Omega_{\text{shield}}$  are made of a silicone-based material Sylgard Q3-3600, whereas the metadvice occupying the annular region  $\Omega_{\text{dev}}$  is made of copper (material A) and polyimide (material B). The thermal properties of the aforementioned materials are given in Tab. 1. The initial

temperature throughout the entire plate is  $T_0 = 273$  K, and the right side temperature is  $T_R = 273$  K. The left side temperature is  $T_L = 313$  K before reaching the first steady regime at  $t_1 = 30000$  s, and it is subsequently increased to  $T_L^* = T_L + \Delta T_L = 313$  K + 10 K = 323 K and maintained until finishing the transient heat conduction analysis at  $t_f = 90000$  s.

Table 1: Thermal properties of Sylgard Q3-3600, copper (material A) and polyimide (material B).

Property	Material		
	Sylgard Q3-3600	Copper	Polyimide
Thermal conductivity [ $\text{W}(\text{mK})^{-1}$ ]	0.77	400	0.17
Volumetric heat capacity [ $\text{J}\cdot\text{m}^{-3}\text{K}^{-1}$ ]	$3.099 \times 10^6$	$3.3495 \times 10^6$	$1.526 \times 10^6$

In the case of a homogeneous plate fully made of Sylgard Q3-3600 (i.e. without the metadvice), the parallel heatlines corresponding to the 1-D heat conduction process depicted

in Fig.3 ( $\mathbf{q}_0 \equiv \mathbf{q}_{\text{hom}}$ ) pass through the circular region to be shielded (white dotted lines) along the entire transient process.

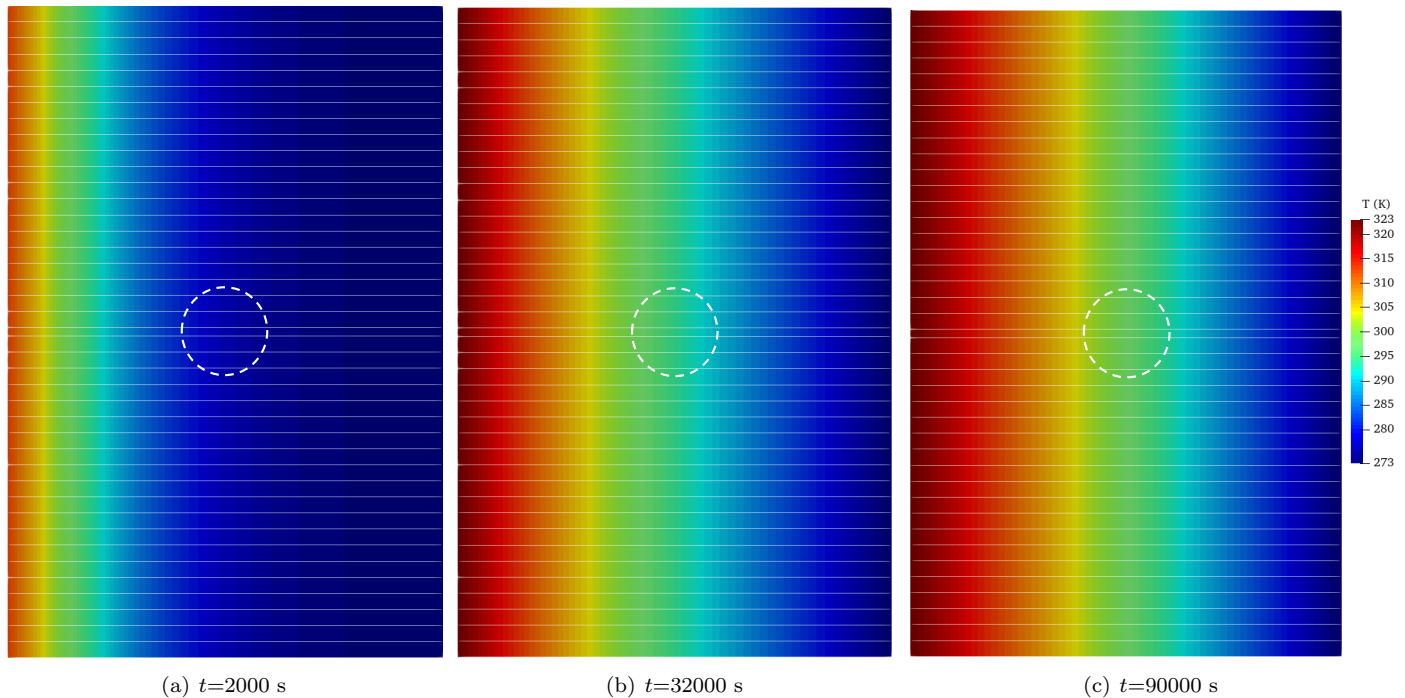


Figure 3: Temperature distribution and heatlines corresponding to the 1-D transient heat conduction in a homogeneous plate made of Sylgard Q3-3600, in the context of Narayana et al. [47] problem.

The proposed TOMD approach is now used to achieve a metadvice conceived to be embedded in the annular region  $\Omega_{\text{dev}}$ , in order to significantly reduce the heat flux passing throughout  $\Omega_{\text{task}} \equiv \Omega_{\text{shield}}$  (delimited by the white dotted lines in Fig.3) along the entire transient heat conduction process. The convergence of the objective function achieved by following the continuation approach explained in section 3 is depicted in Fig.4, which also includes the evolution of

the metadvice topology during the optimisation process. The results reported in this figure demonstrate that using the continuation approach has allowed not only the almost complete suppression of grey zones introduced by the density filter used to eliminate chequerboard-type instabilities, but also a noteworthy improvement of the shielding task fulfilment with respect to the markedly unfeasible design obtained at the first step of the continuation approach ( $\beta = 0$ ).

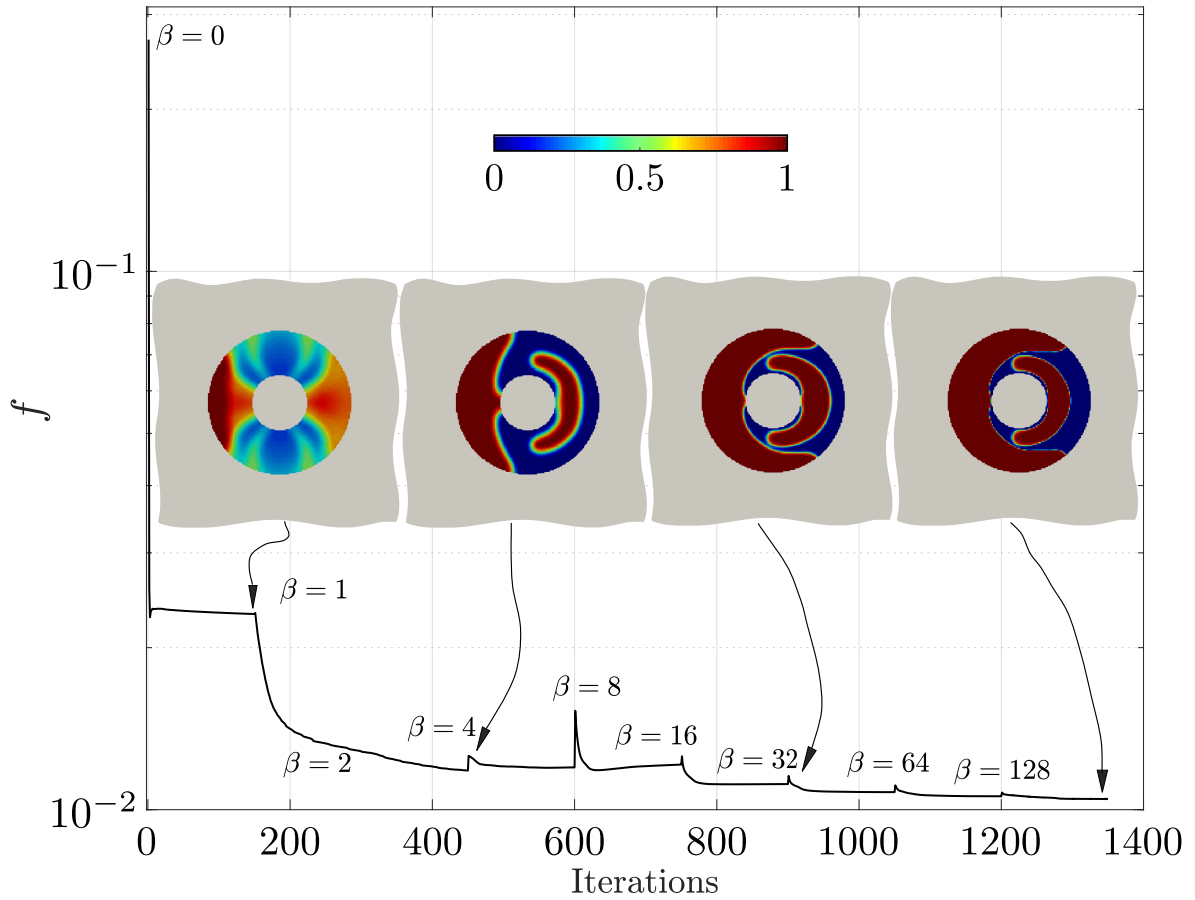


Figure 4: Convergence of the objective function and evolution of topology during the TOMD for heat flux shielding, in the framework of Narayana et al.<sup>[47]</sup> benchmark problem.

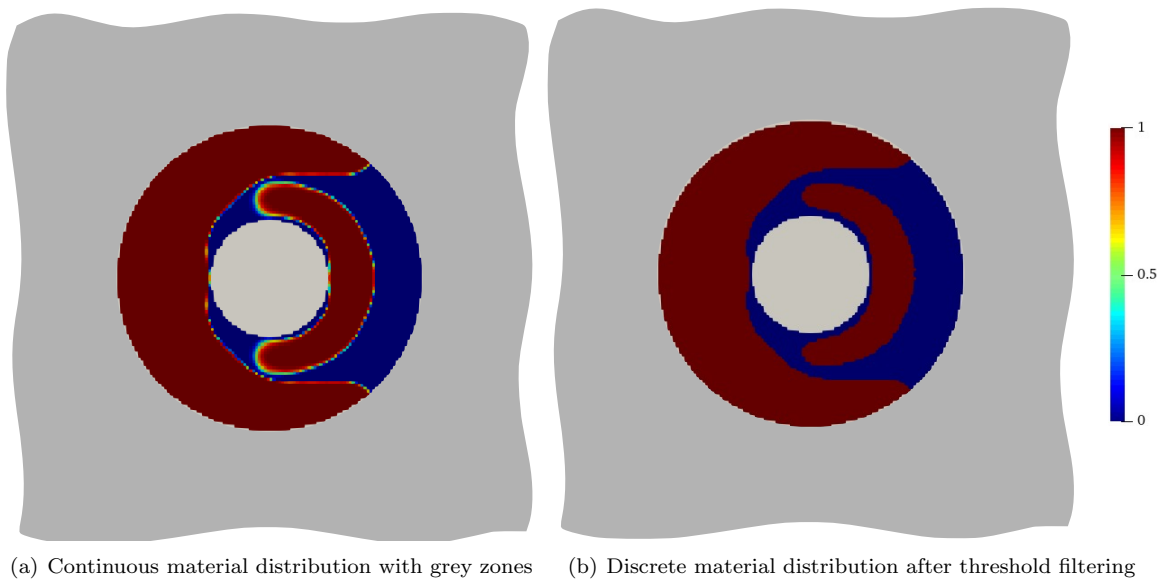


Figure 5: Material distribution obtained after performing the TOMD for heat flux shielding in the context of Narayana et al.<sup>[47]</sup> problem. Copper in blue, polyimide in red, and background material Sylgard Q3-3600 in grey.

The potential of this technique to minimise the objective function while remarkably reducing grey regions has already been demonstrated in classical topological optimisation problems<sup>[58,63,64]</sup>, and this positive feature has now been successfully reproduced in the proposed TOMD framework for transient heat conduction. The continuous (but still unfeasible) material distribution obtained at the last iteration of the optimisation process (enlarged in Fig.5(a)) has allowed a reduction of the objective function up to  $f = 0.0105$ , which means that the time-average mean heat flux passing throughout  $\Omega_{\text{shield}}$  has been reduced by  $(1 - f) \times 100 = 98.95\%$ . Although such a good performance, there are still thin grey regions precluding the metadvice manufacture. The possibility of manufacture is a main concern in this work, whereby the design is now subjected to the final threshold filtering of Eq.32. The  $f^{\text{thr}}/f$  ratio for different thresholds  $w^*$  is plotted in Fig.6, reaching a minimum at  $w^* = 0.8$  where  $f^{\text{thr}}/f = 0.9565$  ( $f^{\text{thr}} = 0.01$ ). This means that the feasible metadvice of Fig.5(b) has enabled a reduction of the time-average mean heat flux passing through  $\Omega_{\text{shield}}$  by 99%, which is even better than the performance achieved using the metadvice of continuous material distribution. Such an outcome is consistent with the convergence behaviour achieved within the continuation approach, where it has been demonstrated that an appropriate removal

of grey regions can actually leads to a better performance of the final design.

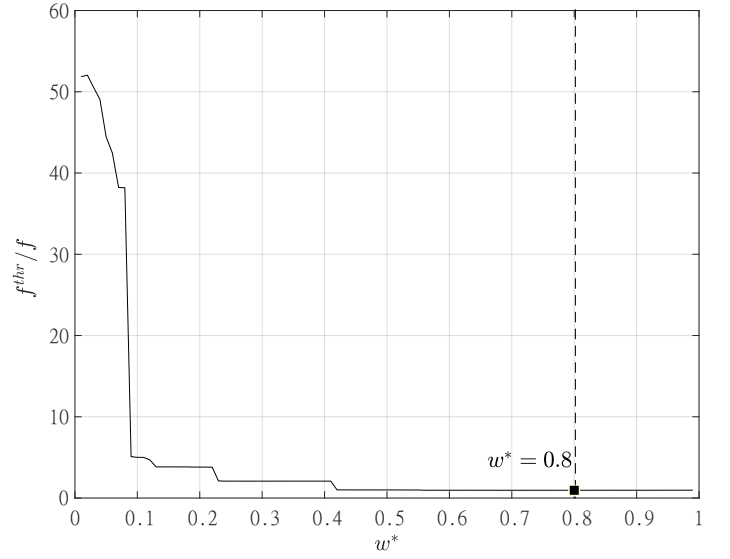


Figure 6: Threshold procedure for the achievement of a feasible heat flux shielding metadvice in the transient heat conduction problem of Narayana et al. <sup>[47]</sup>.

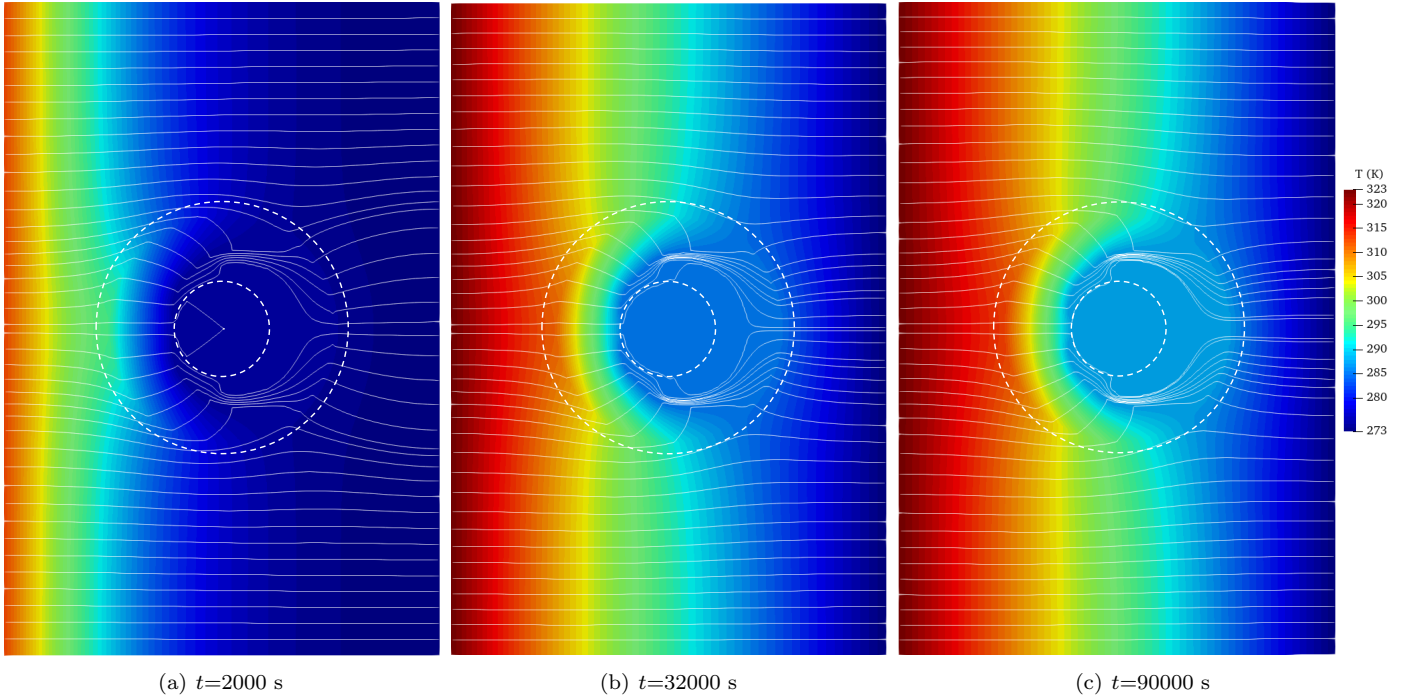


Figure 7: Temperature distribution and heatlines corresponding to the feasible metadvice (after threshold filtering) conceived in the context of Narayana et al. <sup>[47]</sup> problem.

Such an outstanding performance of this feasible metadvice designed via TOMD is depicted in the temperature fields and heatlines resulting from embedding it in the plate,

which are shown in Fig.7 (a)-(c) for different times. Both the temperature field and heat flux are remarkably different from the one-dimensional heat conduction process concern-

ing the case of a homogeneous plate fully made of Sylgard Q3-3600. The way in which the heatlines circumvent  $\Omega_{\text{shield}}$  demonstrates the appropriate performance of the metadvice to fulfil the shielding task, which has also given rise to a noteworthy reduction of temperature in the shielded region during the entire transient heat conduction process. This aspect is put in a better perspective in Fig. 8, where the temperature profiles for different times along the horizontal central axis of the plate are compared to those concerning the case of a homogeneous plate fully made of Sylgard Q3-3600. As discussed in a previous communication<sup>[37,47]</sup>, the reduction of temperature in  $\Omega_{\text{shield}}$  can be seen as a collateral effect of the shielding task fulfilment. Since the metadvice is actually conceived to redirect the heat flux in order to circumvent  $\Omega_{\text{shield}}$  during the entire transient heat conduction process, the total transfer of thermal energy to such region is much smaller and the heating is consequently reduced.

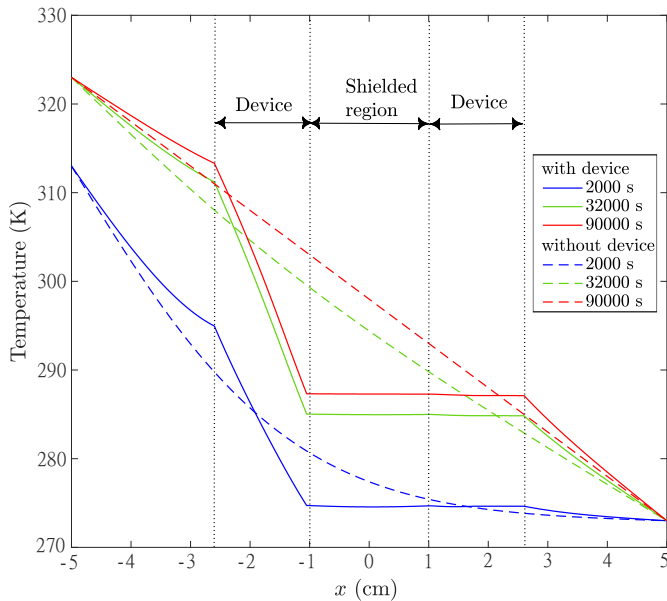


Figure 8: Temperature profiles along the horizontal central axis of the plate with the shielding metadvice designed in the context of Narayana et al.<sup>[47]</sup> problem, compared to those concerning the case of a homogeneous plate fully made of Sylgard Q3-3600.

A comparison between the instantaneous error  $g$  achieved in the transient heat flux shielding task fulfilment when using the metadvice and that concerning the situation of a homogeneous plate fully made of Sylgard Q3-3600  $g_0$  is given in the linear-logarithmic plot of Fig. 9, which depicts the noteworthy reduction of  $g$  with respect to  $g_0$  during the entire transient heat conduction process (even by up to two orders of magnitude). Information of such a kind to quantify the shielding task fulfilment was not provided in the communication of Narayana et. al<sup>[47]</sup>, since the metadvice performance was assessed in terms of the temperature increment  $\Delta T_c$  at the centre of  $\Omega_{\text{shield}}$  from the beginning of the second heating stage ( $t > t_1 = 30,000$  s). The temperature increment at the centre of the plate when using the feasi-

ble metadvice conceived via TOMD is compared in Fig. 10 to that resulting from using the TT and intuition-based metadvice proposed by Narayana et al.<sup>[47]</sup>, which also includes the case without metadvice.

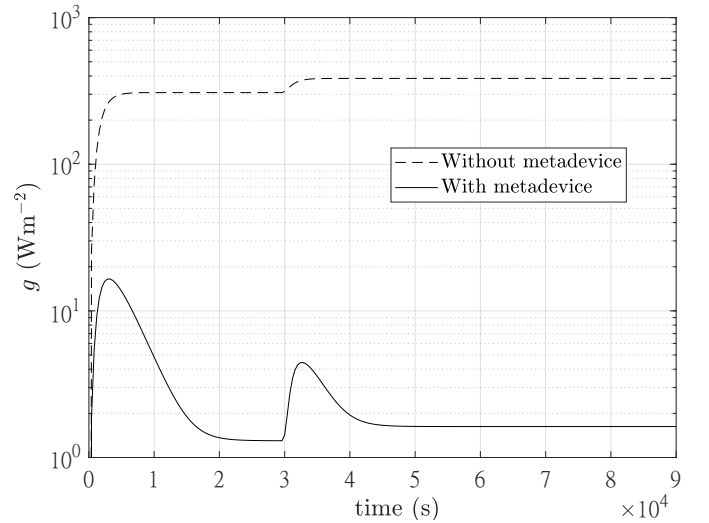


Figure 9: Comparison between the instantaneous error  $g$  achieved in the transient heat flux shielding task fulfilment when using the metadvice and that concerning the situation of a homogeneous plate fully made of Sylgard Q3-3600  $g_0$ .

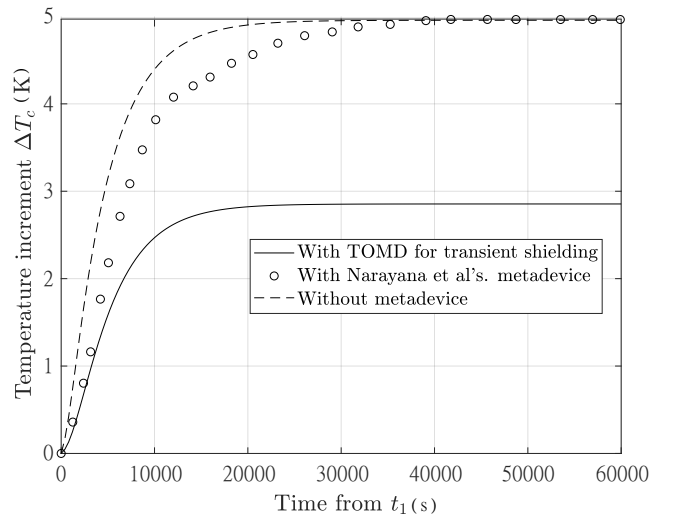


Figure 10: Heating at the centre of the plate for  $t > t_1$  when using both the current TOMD for transient shielding and the metadvice proposed by Narayana et al.<sup>[47]</sup>, and corresponding comparison with the case of a homogeneous plate without shielding device.

Using the heat flux shielding achieved via TOMD has given rise to a heating rate significantly lower than that allowable with Narayana et al.<sup>[47]</sup> device, during the entire transient heat conduction process. Although using the TT and intuition-based metadvice proposed by Narayana et al.<sup>[47]</sup> allows the heating rate at the plate centre to be

slightly reduced, it was unable to prevent the final temperature rise  $\Delta T_c = 5$  K inherent in the case of a homogeneous plate without shielding device. On the other hand, the metadvice achieved via TOMD has allowed a noteworthy reduction of the final temperature rise up to  $\Delta T_c = 2.855$  K. Therefore, both the slower heating rate and lower temperature rise at the plate centre demonstrates the better performance of the current metadvice achieved via TOMD with respect to the TT and intuition-based metadvice proposed by Narayana et al. [47].

#### 4.2. Design, manufacture and experimental assessment of a heat flux shielding metadvice

The geometry in this case is a heterogeneous square plate made of thermal Gad Pad VO (a conformable silicone polymer filled with alumina on a fibreglass carrier) in  $\Omega_{out}$ , with

a central circular region  $\Omega_{shield}$  made of PMMA. The plate has dimensions  $L_x = L_y = 0.1$  m, whereas  $\Omega_{shield}$  has a radius of  $r = 0.01$  m. The region  $\Omega_{dev}$  occupied by the metadvice to be designed to shield the PMMA in  $\Omega_{shield}$  has inner and outer radii  $r = 0.01$  m and  $R = 0.026$  m, respectively. For the TOMD procedure, the FEM-based solution of the governing equations has been performed discretising the upper half of the plate with a uniform mesh of  $200 \times 100 = 20000$  bilinear finite elements. Also in this case, 3614 have their centres within  $\Omega_{dev}$ . Since the artificial density is considered to vary element-wise in  $\Omega_{dev}$ , the resulting non-linear large-scale constrained optimisation problem has 3614 design variables. The metadvice is made of copper (material A) and PMMA (material B), the latter being the same material as that of  $\Omega_{shield}$ . The aforementioned materials are actually those available to the authors for the metadvice manufacture, and the corresponding properties are summarised in Tab. 2.

Table 2: Properties of thermal Gad Pad VO, copper (material A) and PMMA (material B).

Property	Material		
	Thermal Gad Pad VO	Copper	PMMA
Thermal conductivity [W(mK) <sup>-1</sup> ]	0.8	360	0.19
Volumetric heat capacity [J.m <sup>-3</sup> K <sup>-1</sup> ]	$1.6 \times 10^6$	$3.3495 \times 10^6$	$1.526 \times 10^6$

The initial temperature throughout the entire plate is  $T_0 = 293$  K, and the right side temperature is  $T_R = 293$  K. The left side temperature is first increased linearly with time until it reaches  $T_L = 333$  K at 520 s and maintained until a first steady regime is reached at  $t_1 = 10647$  s, and it is subsequently subjected to a further lineal increment to  $T_L^* = T_L + \Delta T_L = 333$  K + 10 K = 343 K at  $t = 10825$  s and maintained until finishing the transient heat conduction analysis at  $t_f = 19500$  s. The temperature fields and heatlines corresponding to the plate without metadvice are

depicted for different times in Fig. 11(a)-(c), which do not correspond to a one-dimensional heat flux case ( $\mathbf{q}_0 \neq \mathbf{q}_{hom}$ ) due to the presence of a different material in  $\Omega_{shield}$  (denoted by the white dotted lines) (PMMA) with respect to the rest of the plate (thermal Gad Pad VO). The convergence of the objective function and evolution of the metadvice topology under the continuation approach used in this work are depicted in Fig.12, achieving also in this case an almost complete suppression of the grey zones together with an improvement of the shielding task fulfilment.

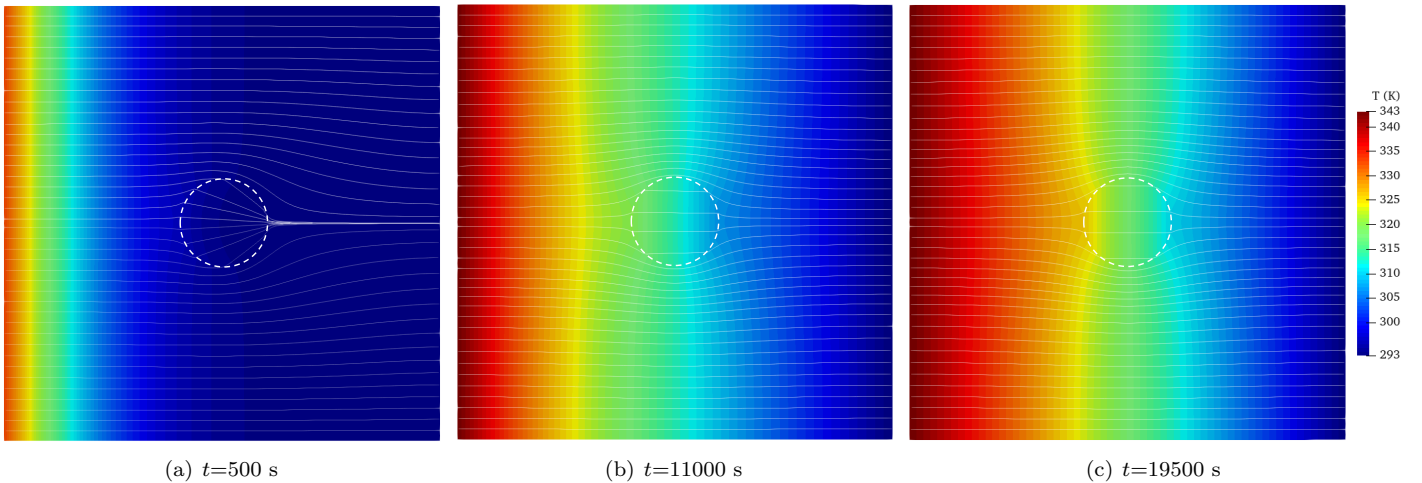


Figure 11: Temperature distribution and heatlines in the heterogeneous plate mostly made of thermal Gad Pad VO, with a PMMA circular inclusion at its centre.

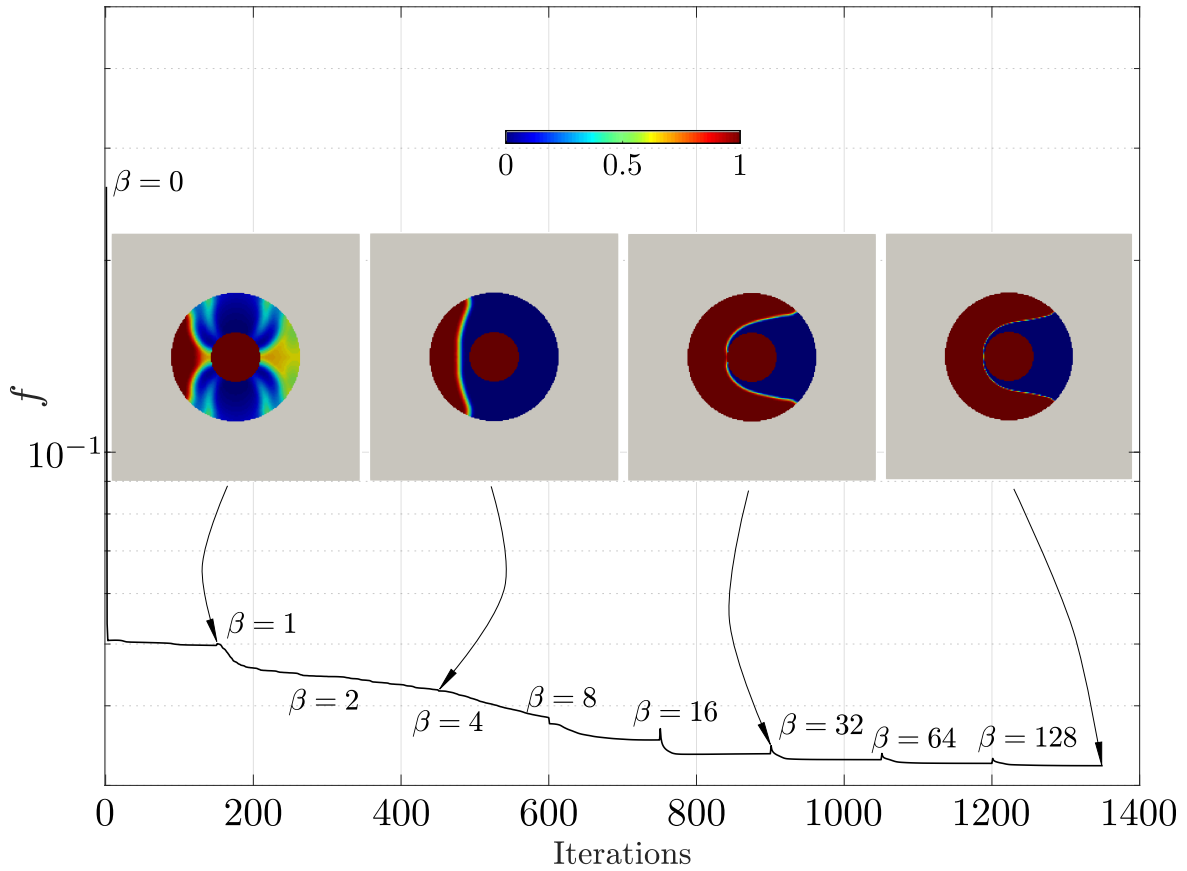


Figure 12: Convergence of the objective function and evolution of topology during the TOMD for heat flux shielding, concerning the metadvice designed to be manufactured and experimentally tested.

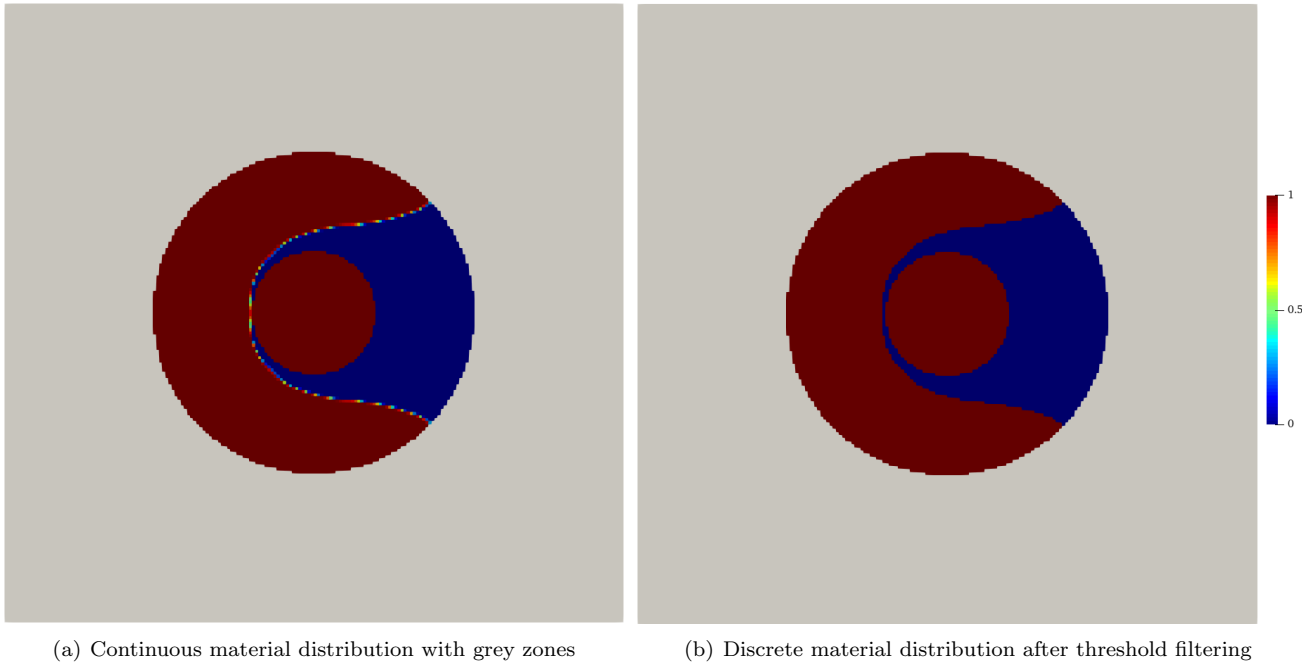


Figure 13: Material distribution obtained via the TOMD approach for the heat flux shielding metadvice to be manufactured. Copper in blue, PMMA in red, and thermal Gad Pad VO in grey.

The metadvice of continuous (but unfeasible) material distribution obtained at the last iteration of the optimisation process (enlarged in Fig.13(a)) allows the objective function concerning the shielding task to be reduced up to  $f = 0.032$ , which means that the time-average mean heat flux passing throughout  $\Omega_{\text{shield}}$  has been reduced by  $(1-f) \times 100 = 96.8\%$ . Also in this case, manufacturability is allowed using the final threshold filtering of Eq.32. The  $f^{\text{thr}}/f$  ratio for different thresholds  $w^*$  is plotted in Fig.14, which exhibits a minimum for  $w^* = 0.97$  where  $f^{\text{thr}}/f = 0.967$  ( $f^{\text{thr}} = 0.031$ ). This means that the resulting feasible metadvice of Fig.13(b) enabled a reduction of the time-average mean heat flux passing throughout  $\Omega_{\text{shield}}$  by 96.9%, which is slightly better than the performance corresponding to the metadvice of continuous material distribution. Also in this case, it is demonstrated that an appropriate removal of grey regions can actually leads to a better performance on the final design. The excellent performance of this metadvice (to be manufactured) is also apparent from the temperature fields and heatlines resulting from embedding it in the plate, which are shown in Fig.15(a)-(c) for different times. The heatlines circumvent  $\Omega_{\text{shield}}$  as a consequence of the shielding task fulfilment by the metadvice, which enables -also in this case- a noteworthy reduction of temperature in the shielding region. The temperature profiles along the horizontal central axis, with and without the metadvice, are given for different times in Fig. 16. Note that the metadvice succeeds to reduce the temperature at  $\Omega_{\text{shield}}$ , as a collateral effect of the shielding task fulfilment. Particularly, at the end of the transient heat conduction process ( $t_f = 19500$  s), the temperature increment has been reduced from  $\Delta T_c = 25$  K

without the metadvice to  $\Delta T_c = 13.44$  K (almost halved) with it. In the linear-logarithmic plot of Fig. 17, the instantaneous error  $g$  achieved in the transient heat flux shielding task fulfilment when using the metadvice is compared to the error  $g_0$  without it. Also in this case, a noteworthy reduction of  $g$  with respect to  $g_0$  during the entire transient heat conduction process (even by up to two orders of magnitude) can be observed.

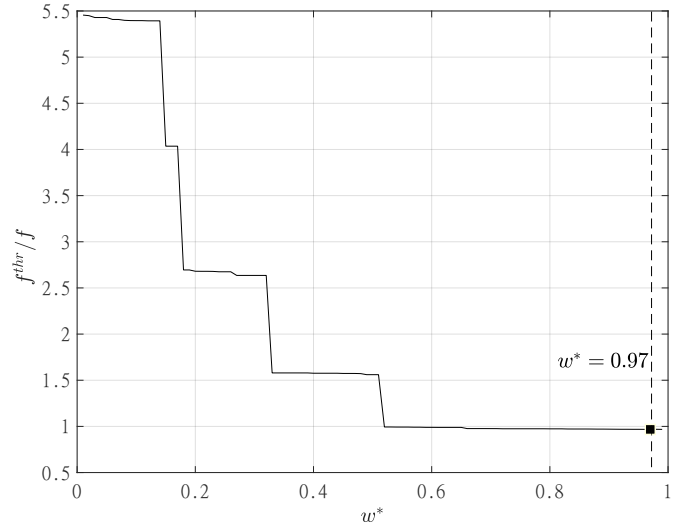


Figure 14: Threshold procedure for the achievement of a feasible final design of the heat flux shielding metadvice to be manufactured and experimentally tested.

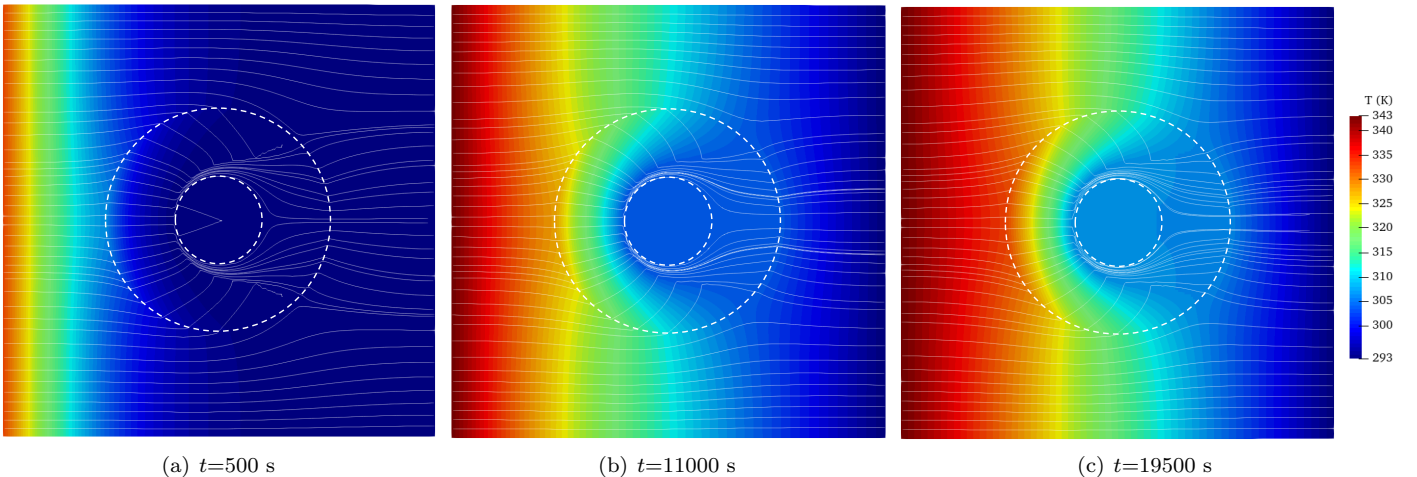


Figure 15: Temperature distribution and heatlines corresponding to the metadvice to be manufactured (after threshold filtering), and conceived to shield the PMMA inclusion in  $\Omega_{\text{shield}}$  from heat flux.

#### 4.2.1. Experimental setup

The experimental measurements of the metadvice thermal performance were conducted at *Laboratoire de Thermique et Énergie, Polytech, Nantes Université*. A scheme

and an actual photo of the experimental setup are shown in Figs. 18(a) and 18(b), respectively. The left and right surfaces of the device were in contact with two aluminium heating plates whose temperatures were controlled using recircu-

lating water flow, whereas polystyrene foam was used as insulator material for the remaining device surfaces. The water temperature of each plate was controlled using two thermostats LAUDA RP 855 during the experiments. The thermostat controlling the hot plate was programmed to achieve the two-steps increasing temperature on the left boundary described in the previous section. The manufactured heat flux shielding metadvice is shown in Fig. 19. The device is 20 mm thick and its remaining dimensions correspond to those reported in the previous section. An appropriate scanning of the temperature distributions with the use of a thermographic camera was not possible, because the different emissivities of the aluminium, thermal Gad Pad VO, copper and PMMA were introducing noteworthy errors in the results obtained. As an alternative, the metadvice performance has been assessed placing thermocouples for temperature data acquisition at different representative locations. As shown in Fig. 19, the metadvice was instrumented with a total of four K-type thermocouples for temperature data acquisition at positions  $Tc_2 - Tc_4$ . Thermocouples  $Tc_2$  and  $Tc_3$  were placed at 22.3 mm and 15.8 mm upstream the shielding region centre ( $O$ ), respectively. Thermocouple  $Tc_4$  was placed at  $\Omega_{\text{shield}}$  centre, and  $Tc_5$  16 mm downstream  $O$ .

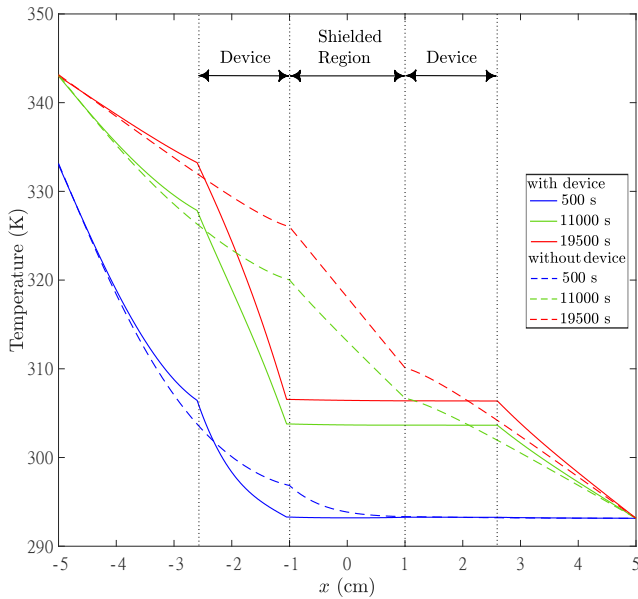


Figure 16: Temperature profiles along the horizontal central axis of the plate with the heat flux shielding metadvice to be manufactured, compared to those of the thermal Gad Pad VO plate with a PMMA inclusion at its centre (without metadvice).

Two additional thermocouples  $Tc_1$  and  $Tc_6$  were used to verify the appropriate setting of temperature at the left and right boundaries (device-plates interfaces), respectively. The metadvice parts were designed and manufactured with a sliding tolerance so that it can be assembled manually by applying a small force. Additionally, a highly conductive grease was applied at the contact surfaces to emulate perfect heat transfer between the parts.

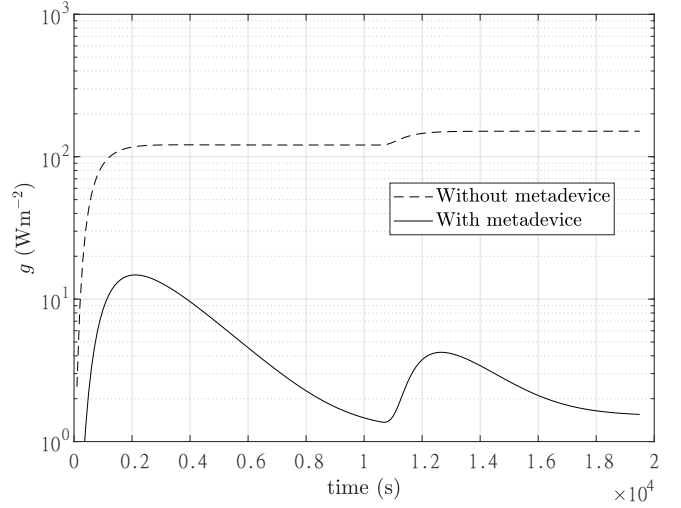
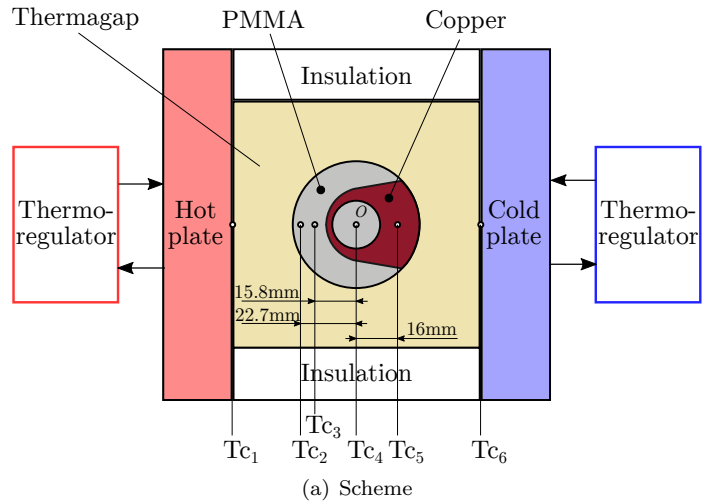
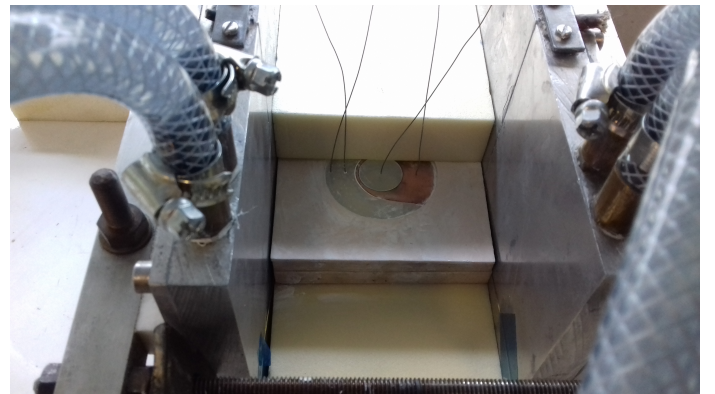


Figure 17: Instantaneous error  $g$  achieved in the transient heat flux shielding task fulfillment when using the metadvice to be manufactured, compared to the error  $g_0$  without metadvice.



(a) Scheme



(b) Actual picture

Figure 18: A scheme and a photo of the experimental setup used to assess the thermal performance of the heat flux shielding metadvice.

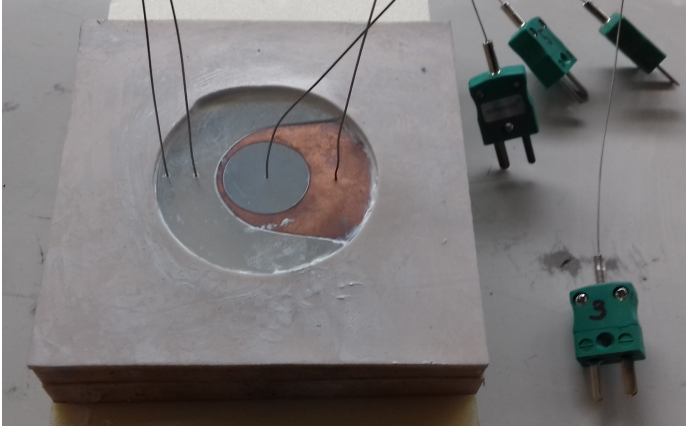


Figure 19: The manufactured heat flux shielding device instrumented with four K-type thermocouples.

#### 4.2.2. Validation of numerical results with experiments

In Fig. 20, the temperature-time data collected at  $T_{c_4}$  (the centre of  $\Omega_{\text{shield}}$ ) is compared to the temperature predicted at the same position via FEM-based numerical solutions for the cases with and without metadvice.

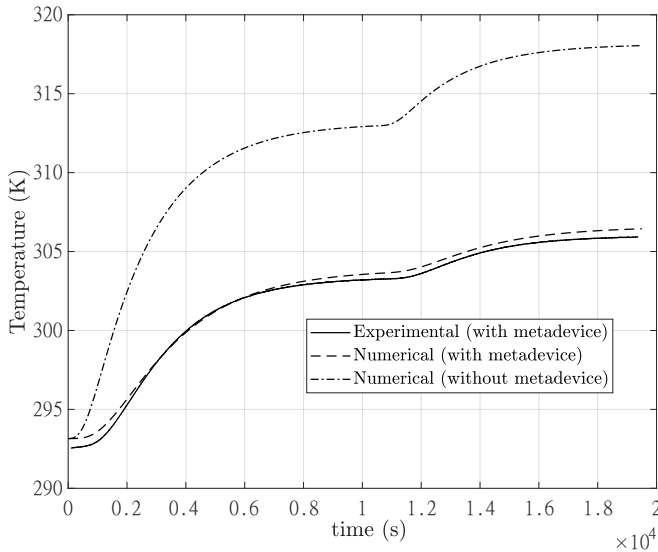


Figure 20: Validation of the numerical prediction of temperature at the centre of  $\Omega_{\text{shield}}$ , by comparison of temperature data collected at  $T_{c_4}$  with FEM-based numerical solutions.

The actual thermal performance of the metadvice exhibits an excellent agreement with the FEM-based numerical solutions, and the results also demonstrate that using the metadvice gives rise to a noteworthy reduction of heating at the centre of  $\Omega_{\text{shield}}$ . The maximum discrepancies between the numerical and experimental results during the transient analysis has been only about 0.5 K, with the experimental temperature measurements being slightly below the numerical results. Despite the controlled conditions of the experiment, it is also subjected to some sources of error

such as the non-perfect isolation of the surfaces intended to be adiabatic, the contact between the metadvice parts and that of the aluminium plates with the left and right surfaces, and the inherent uncertainty of the data acquisition with the thermocouples.

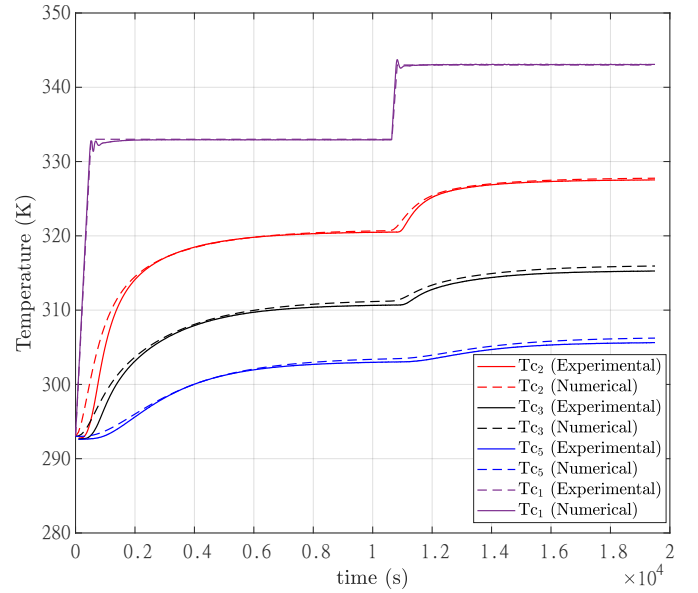


Figure 21: Validation of the numerical prediction of temperature at the position of thermocouples  $T_{c_1} - T_{c_3}$  and  $T_{c_5}$ , by comparison of temperature data collected at the thermocouples with FEM-based numerical solutions.

Despite having set up the experiment so that the device had a uniform initial temperature of 293 K, the data obtained with the thermocouple has exhibited slightly lower values (approximately 292.5 K) at the initial transient. The metadvice has not yet undergone sufficient conduction heating effects from the left surface at these early stages, with the consequence of a slight decrease in temperature due to small heat losses (non-perfect isolation at surfaces intended to be adiabatic). The effects of heat losses are attenuated as the transient conduction process proceeds and the centre of the plate experiences higher heating rates, with the consequence of a temporary reduction of the discrepancies between the experimental values and the ideal numerical simulation. The effect of heat losses becomes noticeable as the heat conduction process approaches the steady state, again leading to a slight discrepancy between the experimental results and the numerical solution. A comparison of the FEM-based solutions with the temperature data collected by the remaining thermocouples is depicted in Fig.21, exhibiting an excellent matching also in such locations. These results also exhibit slight discrepancies (less than 0.5 K) between the experimental values and the numerical solutions for the thermocouples located at the metadvice, which are also explained by the interaction between the heat losses and the heating rate effects.

## 5. Discussion

The results reported in the previous section have been useful to prove the noteworthy potential of the TOMD procedure to achieve feasible thermal metadivices for manipulation of conductive heat flux in transient regime, considering the particular case of a heat flux shielding task. Given the higher thermal gradients upstream the shielding region during most of the transient heat conduction process, the metadivices designed using the proposed approach exhibit an unsymmetrical material distribution with respect to the  $y$ -axis. The metadivices designed either to be compared with the classical TT method or to be fabricated and tested mostly dispose of the material with the lowest conductivity and volumetric heat capacity upstream of the shielding region (Figs. 3 and 9), hindering the heat flux towards such area and increasing the thermal gradients along  $x$  direction (Figs. 5 and 11). Both metadivices have the material with the highest conductivity and volumetric heat capacity near and downstream of  $\Omega_{\text{shield}}$ , allowing the heat absorbed upstream the shielding region to flow subsequently circumventing it. With regard to the device designed to be compared with the TT- and intuition-based Narayana et al.'s shielding device<sup>[47]</sup>, the proposed TOMD technique has lead to a metadivice exhibiting a noteworthy better performance. On the other hand, the excellent matching between the experimental and numerical results concerning the metadivice designed and manufactured with materials available in laboratory demonstrated the actual possibility of using the TOMD to manipulate heat flux in a realistic scenario. Such outcomes demonstrate the significance of developing a specific procedure for the achievement of a thermal metadivice designed to accomplish a given task under transient conditions. In this sense, the TOMD approach leads to the design of a thermal metadivice conceived to shield the heat flux in terms of the instantaneous temperature distributions before the steady-state condition is reached, i.e. the heat flux is properly shielded during the entire heat conduction process. The good performance of the metadivices designed for the two cases addressed in this work also demonstrates the reliability and suitability of the TOMD to properly fulfil transient heat flux manipulation tasks, with the versatility of allowing the design of an easy-to-make metadivice for each particular transient heat conduction scenario. The TOMD reported so far in the literature are -to the authors' best knowledge- limited to heat flux manipulation and thermal cloaking in steady regime, regardless the implementation of density-based<sup>[15,43,44]</sup> or level set-based<sup>[7,10,11,19–21]</sup> procedures. Such designs are dictated in terms of only the search for an appropriate distribution of thermal conductivity to fulfil a given heat flux manipulation task, whereas Narayana et al.<sup>[47]</sup> and Álvarez-Hostos et al.<sup>[37]</sup> have already demonstrated that the appropriate design of a metadivice to perform a transient heat flux manipulation task must be dictated in terms of a proper spatial arrangement of both the thermal conductivity and the volumetric heat capacity.

Although the metadivices designed in this work have exhibited a very good performance in the fulfilment of the shielding task, the instantaneous error  $g$  in both cases addressed in this communication (Fig. 6 and 12) indicates the entrance of some heat flux into the shielding region at the beginning of each transient stage during the heat conduction process. This is because these stages are the most critical for the shielding task fulfilment as a consequence of the sudden increase of the left boundary temperature at the initial transient. However, the results demonstrate that the performance achieved via TOMD at this stage is still much better than that of TT- and intuition-based devices. Furthermore, the successful use of the TOMD approach in two different scenarios demonstrates the versatility of this technique to accommodate the metadivice design (and, consequently, the distribution of thermal properties) according to the available candidate materials, and the conditions of the transient heat conduction process. This is a significant improvement over the design of metadivices via TT, where there is a pressing and limiting need to search for specific materials that emulate -at least approximately- the distribution of thermal properties prescribed by the coordinate transformations procedure. Summarising, the devices conceived via TOMD are not only easy-to-make since they are based on macroscopically distinguishable isotropic candidate materials, but they also perform the heat flux shielding task significantly better than those achieved via TT and intuition. It is important to remark that the superior performance of this TOMD approach for transient applications is strongly linked to the unsymmetrical material distribution with respect to the  $y$ -axis, which is not observed either in TOMD for steady applications or the distribution of thermal properties achieved using TT for transient applications. The reason for this in the TOMD for steady applications is that the optimisation problem is formulated only in terms of the temperature distribution achieved once the steady regime has been reached, and the material distribution is dictated by the thermal conductivity<sup>[10,11,15,43,44]</sup>. On the other hand, the distribution of thermal properties concerning the TT approach is achieved mapping the homogeneous plate temperature field within  $\Omega_{\text{dev}} \cup \Omega_{\text{shield}}$  into the annular domain of the metadivice  $\Omega_{\text{dev}}$ , regardless the temperature field in  $\Omega_{\text{out}}$ <sup>[34,47]</sup>. This has the consequence of setting a homogeneous thermal field (null heat flux) in  $\Omega_{\text{shield}}$ , which matches the temperature at the plate centre before the coordinates transformation. The features discussed so far in relation to the distribution of thermal properties achieved in the context of both TOMD for steady heat flux manipulation and TT for transient heat conduction demonstrate that such approaches are conceived without considering the effects of having thermal gradients upstream  $\Omega_{\text{shield}}$  being higher than those downstream  $\Omega_{\text{shield}}$ , in the course of the whole transient heat conduction process. Such aspect explains the impossibility of having a reduction of heating at the plate centre as a secondary consequence of fulfilling the shielding task. This is a feature where the TOMD specifically proposed in this work for transient heat flux manipulation has exhibited a noteworthy superior performance,

since the metadevices conceived under this procedure have allowed a significant reduction of temperature in the shielding region. The reason for this outcome is that the TOMD approach proposed in this work is specifically formulated to shield the heat flux considering the entire thermal history of the transient heat conduction process, i.e. the effects of having thermal gradients upstream  $\Omega_{\text{shield}}$  being higher than the downstream  $\Omega_{\text{shield}}$  are not neglected. This does not only have the consequence of achieving a homogeneous temperature distribution in  $\Omega_{\text{shield}}$  (shielding), but also of redirecting the heat flux to reduce the total transfer of thermal energy to the shielding region.

### 5.1. Performance of multiple tasks and significance of designing for transient regime

Although the proposed density-based TOMD procedure for transient heat flux manipulation has been so far implemented for the particular task of shielding, its extension to perform different heat flux manipulation tasks is straightforward (as discussed in section 2.3.). The metadevices achieved so far have been conceived to merely fulfil the shielding task in  $\Omega_{\text{shield}} = \Omega_{\text{in}}$ , regardless the perturbations introduced in the temperature distribution and conductive heat flux in  $\Omega_{\text{out}}$ . The current section is devoted to demonstrate the versatility of the current TOMD approach to perform the simultaneous fulfilment of different tasks, considering the particular example of simultaneous heat flux shielding and thermal cloaking. Starting from the TOMD for heat flux shielding performed in the context of Narayana et al.'s benchmark problem<sup>[47]</sup>, the TOMD will now be conducted to additionally perform a cloaking task in  $\Omega_{\text{out}}$ . The metadvice must now be designed to shield the heat flux

( $\bar{\mathbf{q}} = \mathbf{0}$ ) in  $\Omega_{\text{shield}} \equiv \Omega_{\text{task1}} = \Omega_{\text{in}}$ , while keeping unaltered the heat flux ( $\bar{\mathbf{q}} = \mathbf{q}_{\text{hom}}$ ) in  $\Omega_{\text{cloak}} \equiv \Omega_{\text{task2}} = \Omega_{\text{out}}$ . It is worth to mention that this metadvice designed for simultaneous fulfilment of the thermal cloaking and heat flux shielding tasks is also often referred as perfect thermal cloaking shell or cloak<sup>[16,20,34,45]</sup>, which is different from classical cloaking metadevices merely conceived to control heat flux making the temperature field around an object or inclusion in a homogeneous media behave as if it is not there (shielding is not performed)<sup>[7,8,19–21]</sup>. Thus the objective function given in (13) is now computed considering the following root mean square error in the simultaneous fulfilment of the thermal cloaking and heat flux shielding tasks at a given time  $t$ :

$$g(\mathbf{P}, t) = \omega \times g_1(\mathbf{P}, t) + (1 - \omega) \times g_2(\mathbf{P}, t), \quad (33)$$

with  $g_1(\mathbf{P}, t)$  given as

$$g_1(\mathbf{P}, t) = \left[ \frac{1}{\sum_{h_1=1}^{H_1} \Delta\Omega_{h_1}} \sum_{h_1=1}^{H_1} \|\mathbf{q}(\mathbf{P}, \mathbf{x}_{h_1}, t)\|^2 \Delta\Omega_{h_1} \right]^{1/2}, \quad (34)$$

and  $g_2(\mathbf{P}, t)$

$$g_2(\mathbf{P}, t) = \left[ \frac{1}{\sum_{h_2=1}^{H_2} \Delta\Omega_{h_2}} \sum_{h_2=1}^{H_2} \|\mathbf{q}(\mathbf{P}, \mathbf{x}_{h_2}, t) - \mathbf{q}_{\text{hom}}(\mathbf{x}_{h_2}, t)\|^2 \Delta\Omega_{h_2} \right]^{1/2}, \quad (35)$$

where  $H_1$  is the number of elements  $\Delta\Omega_{h_1} \in \Omega_{\text{in}}$  with centre  $\mathbf{x}_{h_1}$ , whereas  $H_2$  is the number of elements  $\Delta\Omega_{h_2} \in \Omega_{\text{out}}$  with centre  $\mathbf{x}_{h_2}$ . The multipliers  $\omega$  and  $1 - \omega$  (with  $0 \leq \omega \leq 1$ ) are the weights assigned to the fulfilment of shielding and cloaking tasks, respectively.

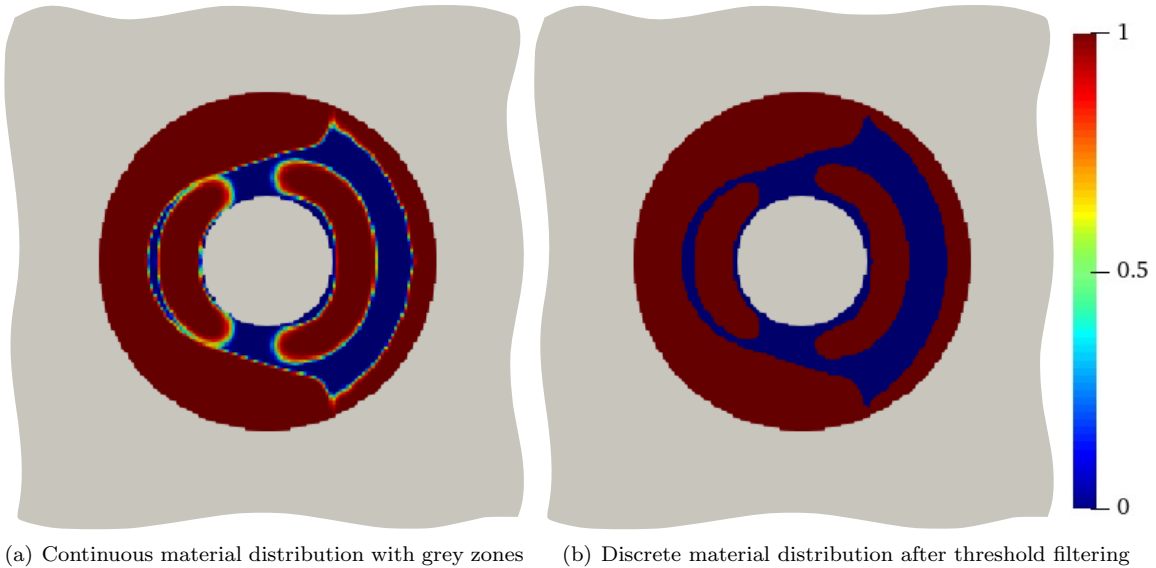


Figure 22: Material distribution obtained after performing the TOMD for simultaneous heat flux shielding and thermal cloaking, in the context of Narayana et al.<sup>[47]</sup> problem. Copper in blue, polyimide in red, and background material Sylgard Q3-3600 in grey.

This weighted definition of the objective function has already been used in a previous communication on microparameters-based OMD for transient heat flux manipulation, and also implemented by Nakagawa et. al<sup>[20]</sup> in the level set-based TOMD for steady heat flux manipulation. The TOMD has been performed with  $\omega = 0.5$ , and the resulting continuous and threshold filtered materials distribution concerning the metadvice for simultaneous heat flux shielding and thermal cloaking are depicted in Fig.22. This metadvice design has been performed following the same continuation procedure and final threshold filtering used so far in this communication, whose convergence features for the achievement of a final feasible material arrangement have already been demonstrated in the design of two metadvice for pure heat flux shielding. The effects of the feasible metadvice (after threshold filtering) of Fig.22(b) on both temperature distribution and heatlines are depicted in Fig.23. Such results demonstrate that the current metadvice has not only performed the shielding task, but it has also done so in a way that limits the conductive heat flux disturbances in  $\Omega_{\text{out}}$ . It is also worth to note that the metadvice exhibits some difficulties to fulfil the assigned tasks at the early stages of the transient heat conduction process, as occurred in the case of the pure heat flux shielding metadvice designed in the previous sections. Also for the cloaking task, these stages are the most critical due to the sudden increase of the left boundary temperature at the initial tran-

sient. This metadvice has allowed a reduction of objective function up to  $f^{\text{thr}} = 0.0138$ , with the shielding task fulfilled up to  $f_1^{\text{thr}} = 0.0122$ . This means that the time-average mean heat flux passing through  $\Omega_{\text{shield}}$  has been reduced by 98.78%, which is a detriment of only  $99\% - 98.78\% = 0.22\%$  with respect to the metadvice purely conceived for transient heat flux shielding (Fig.5). This result is actually consistent with outcomes of previous communications on density-based TOMD for steady-state heat flux manipulation<sup>[44]</sup> and mechanical cloaking<sup>[28]</sup>, and microparameters-based OMD for thermo-mechanical<sup>[30]</sup> cloaking and for heat flux manipulation in transient regime<sup>[37]</sup>. In the aforementioned works, metadvice designed for multiple tasks have exhibited a slight detriment on its performance when compared in a single task with others specifically designed to fulfil only such a particular task. A better perspective on the fulfilment of the thermal cloaking task is given in the plot of Fig.24, which depicts the value of the normalised root mean square error ( $\text{RMSE}_{\text{cloak}}$ ):

$$\text{RMSE}_{\text{cloak}}(\mathbf{P}, t) = \left[ \frac{\int_{\Omega_{\text{out}}} \|\mathbf{q}(\mathbf{P}, \mathbf{x}, t) - \mathbf{q}_{\text{hom}}(\mathbf{x}, t)\|^2 d\Omega}{\int_{\Omega_{\text{out}}} \|\mathbf{q}_{\text{hom}}(\mathbf{x}, t)\|^2 d\Omega} \right]^{1/2} \quad (36)$$

in the case of using both the metadvice conceived only for heat flux shielding and the current one designed for simultaneous thermal cloaking and heat flux shielding.

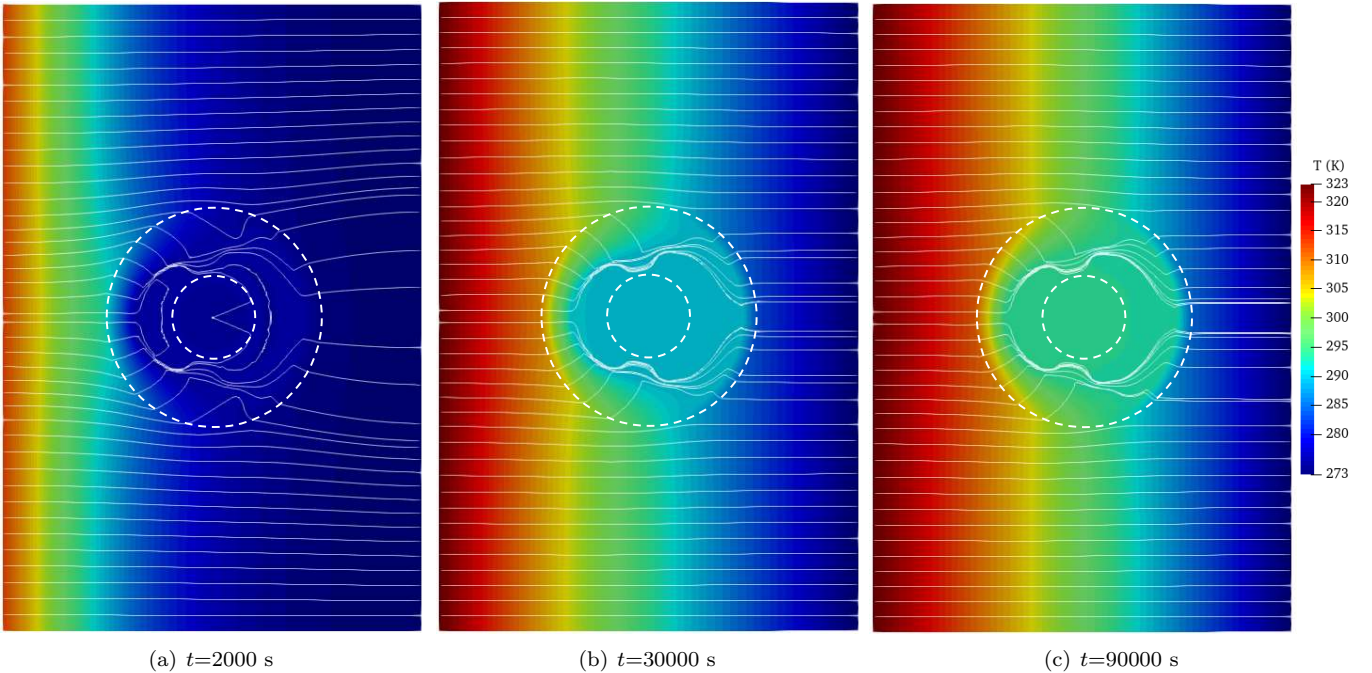


Figure 23: Temperature distribution and heatlines corresponding to the feasible metadvice (after threshold filtering) for simultaneous heat flux shielding and thermal cloaking, conceived in the context of Narayana et al.<sup>[47]</sup> benchmark problem.

Using the metadvice for pure heat flux shielding has globally perturbed the heat flux in  $\Omega_{\text{out}}$  by more than 12% during most of the transient heat conduction process, with a maximum discrepancy with respect to  $\mathbf{q}_{\text{hom}}$  of ap-

proximately 14% during the initial transient. The current metadvice conceived for simultaneous heat flux shielding and thermal cloaking has enabled the mitigation of such perturbations to less than 2% during most of the transient

heat conduction process, with a maximum discrepancy with respect to  $\mathbf{q}_{\text{hom}}$  of almost 6% at  $t = 2000$  s. Such time instant correspond to the heatlines and temperature distributions depicted in Fig.23(a), which still exhibit perturbations in  $\Omega_{\text{out}}$  with respect to the case of a plate fully made of the background material Sylgard Q3-3600. The temperature profiles along the horizontal central axis, with and without the metadvice, are given for different times in Fig. 25.

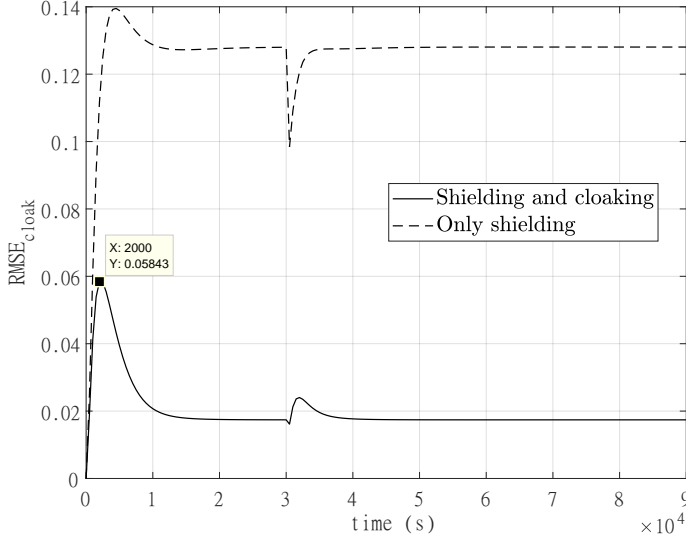


Figure 24: RMSE in the fulfilment of the cloaking task, during the entire transient heat conduction process

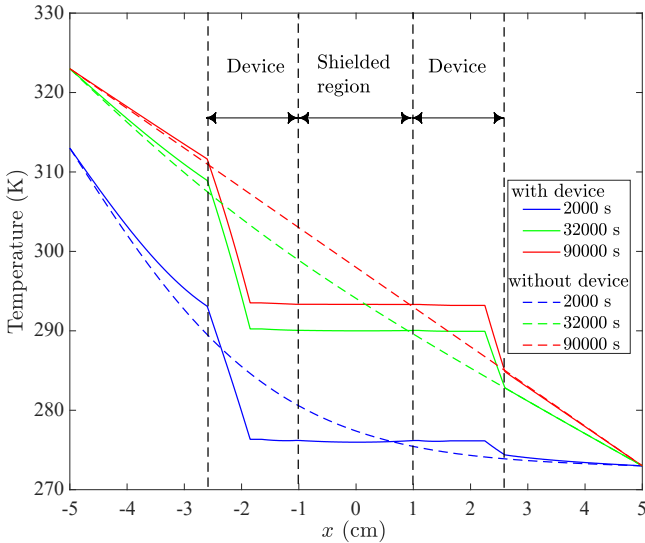


Figure 25: Temperature profiles along the horizontal central axis of the plate with the metadvice designed for simultaneous heat flux shielding and thermal cloaking, compared to those concerning the case of a homogeneous plate fully made of Sylgard Q3-3600.

The metadvice have succeeded in achieving both virtually null thermal gradients in  $\Omega_{\text{shield}}$  and a good match-

ing with the temperature profiles corresponding to the homogeneous plate in  $\Omega_{\text{out}}$ , which have exhibited significant discrepancies when using the device designed for pure heat flux shielding (Fig.5). The main concern of this work is to demonstrate the significance of an appropriate assessment of temperature variations in the TOMD for heat flux manipulation in transient regime, which –to the authors’ best knowledge– has not yet been properly addressed in the revised literature. This can be put in a better perspective comparing the performance of the metadvice designed in this work via TOMD in transient regime, to another metadvice designed under a formulation particularly developed for heat flux manipulation in the steady state<sup>[42–44]</sup>. The material distribution achieved via TOMD for heat flux shielding in steady state is depicted in Fig.26, which is also obtained performing the continuation procedure and further threshold filtering. Applied to the transient problem described in Section 4.1., the feasible metadvice of Fig.26(b) has allowed a reduction of the objective function up to  $f^{\text{thr}} = 0.0134$ . This value is 1.34 times that corresponding to the TOMD performed in transient conditions for pure heat flux shielding, and 1.1 times that corresponding to the TOMD performed in transient conditions for simultaneous heat flux shielding and thermal cloaking. This metadvice conceived under a pure steady analysis has reduced the heat flux passing throughout  $\Omega_{\text{shield}}$  during the transient heat conduction process up to  $(1 - f^{\text{thr}}) \times 100 = 98.66\%$ , which represents a slight detriment with respect to the metadvice achieved when considering appropriately the transient effects in the TOMD procedure. The symmetry of the material distribution depicted in Fig.26 is actually a direct consequence of having designed the metadvice with a heat flux shielding task prescribed in steady regime<sup>[20,37,44]</sup>, which has already been demonstrated to degrade their performance in such a task at the early stages of transient heat conduction processes due to higher thermal gradients upstream  $\Omega_{\text{shield}}$ <sup>[37]</sup>. The behaviour achieved on the root mean square error  $g$  concerning the instantaneous fulfilment of the transient heat flux shielding task is depicted in Fig.27 for the cases of: (i) The metadvice specifically designed for heat flux shielding in transient regime (Section 4.1, Fig.5), (ii) The metadvice designed for simultaneous heat flux shielding and thermal cloaking in transient regime (Fig.22), and (iii) The metadvice specifically designed for heat flux shielding in the framework of an over-simplified steady-state analysis (Fig.26). The metadvice designed in the framework of transient analyses exhibit the best performance before reaching the steady-state, even in the case of demanding simultaneous cloaking. It is also worth note that the metadvice based on the over-simplified steady-state analysis performs better under the conditions for which it is actually conceived, i.e. shielding the heat flux concerning a stable temperature distribution. This has actually a direct consequence on the heating in  $\Omega_{\text{shield}}$ , which is depicted in the time-temperature plot given in Fig.28 for the plate centre. The metadvice specifically conceived to perform the shielding task in transient regime has enabled the reduction of both heating rate and maximum temperature reached at the plate centre, even

if such features are degraded as a consequence of demanding the simultaneous fulfilment of the thermal cloaking task. This has not been possible with the pure heat flux shielding

device based on a steady-state analysis, which has given rise to a behaviour very similar to the case of the homogeneous plate.

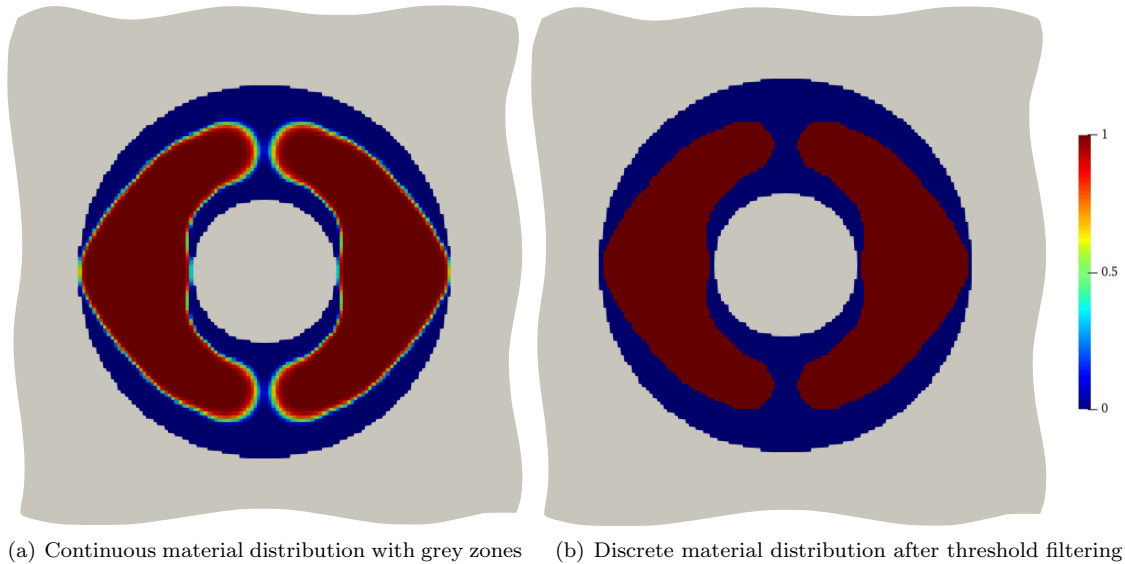


Figure 26: Material distribution obtained after performing the TOMD for steady heat flux shielding. Copper in blue, polyimide in red, and background material Sylgard Q3-3600 in grey.

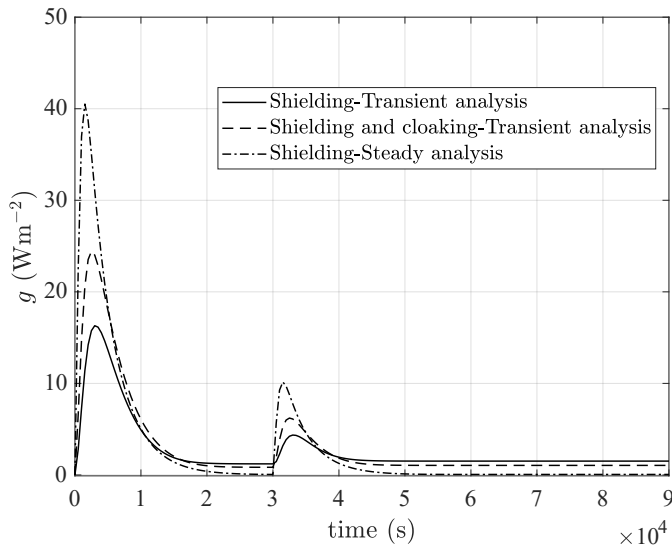


Figure 27: Behaviour of the root mean square error  $g$  concerning the heat flux shielding task fulfilment, according to the procedure used for the TOMD.

This is because such a metadvice does not properly perform the heat flux shielding task during the heating, but once a stable temperature distribution is achieved. The outcomes reported so far put in a very clear perspective the significance of metadvice specifically designed to manipulate heat flux in transient regime, which in this communication has been performed via TOMD to ensure easy manufactura-

bility. Even demanding thermal cloaking in addition to heat flux shielding, a metadvice designed under an appropriate transient analysis has exhibited a better performance than a pure heat flux shielding metadvice conceived in the framework of a steady analysis.

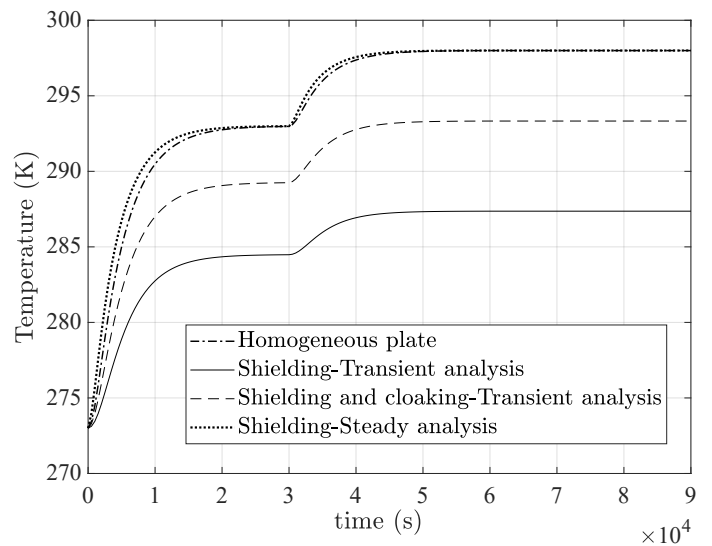


Figure 28: Behaviour of temperature at the centre of  $\Omega_{\text{shield}}$ , according to the procedure used for the TOMD.

## 6. Conclusions

A novel approach for the design and manufacture of thermal metadevices for heat flux manipulation in transient regime has been introduced. This approach has involved the solution of a large scale topology optimisation problem, where the objective function to be minimised is defined in terms of the error in fulfilling a heat flux manipulation task prescribed along a time period of the transient heat conduction process. The procedure is conceived to achieve easy-to-make metadevices made of two macroscopically distinguishable isotropic materials with highly contrasting thermal conductivity and volumetric heat capacity, and the solid isotropic material with penalisation (SIMP) technique has been used to define the material distribution as a continuous function. Using the shielding task as an example, the proposed topology optimisation-based metadvice design (TOMD) has been used in two different scenarios. A first metadvice has been designed to compare its performance to another conceived via the classical transformation thermodynamics (TT) technique and intuition, in the context of the same transient heat conduction problem. The TOMD approach has promoted an unsymmetrical material distribution to preserve the shielding region from the high thermal gradients upstream of it, leading to a better performance in the shielding task compared to the device based on TT and intuition. Such a superior performance has been reflected in both the slower heating rate and lower temperature rise in the shielding region, being the last feature unfeasible with the metadvice conceived via TT and intuition. The unsymmetrical material distribution promoted by the proposed TOMD procedure in the problems addressed is actually a consequence of properly considering the transient effects to fulfil the shielding task, which is a feature exhibited neither by the device based on TT and intuition nor metadevices also designed via topology optimisation but with the shielding task prescribed in steady regime. A second metadvice has also been designed using candidate materials available to the authors, allowing its actual manufacture with pieces of easy manual assembly. Such metadvice has also allowed a very good fulfilment of the shielding task, and its performance has been validated experimentally. The actual thermal behaviour of the metadvice during experimentation has exhibited an excellent agreement with the performance predicted in the FEM-based numerical simulations, achieving also in this case a slower heating rate and lower temperature rise in the shielding region. These outcomes concerning the second metadvice not only have demonstrated the actual potential of the TOMD to manipulate heat flux in a realistic scenario, but also the possibility of excelling the performance of TT-based metadevices without being limited to a single set of candidate materials. The first metadvice was obtained using copper and polyimide to shield a region made of Sylgard Q3-3600 (the same materials set used in the TT and intuition-based metadvice proposed by Narayana et al.<sup>[47]</sup>), whereas the second metadvice consisted of an arrangement of copper and PMMA to shield an inclusion

of PMMA in a plate made of thermal Gad Pad VO. Both metadevices have allowed significantly slower heating rates and a lower temperature rise in the shielding region, which -to the authors' best knowledge- has so far not been possible with devices based on coordinate transformation. Additionally, such an outstanding performance has been achieved without the restrictive need to limit the candidate materials to those that can emulate -at least approximately- the properties dictated by TT techniques.

The versatility of the proposed TOMD for transient heat flux manipulation was also finally proven in the design of a metadvice for simultaneous heat flux shielding and thermal cloaking, where it has been proven that the collateral fulfilment of the thermal cloaking outside the metadvice is detrimental to the main purpose of heat flux shielding. Such an aspect has supported another noteworthy advantage with respect to the TT-based approaches, where cloaking outside the device is always imposed irrespectively of the main heat flux manipulation task.

## References

- [1] Wenshan Cai and Vladimir Shalaev. *Optical Metamaterials*. Springer New York, 2010.
- [2] Miles V. Barnhart, Xianchen Xu, Yangyang Chen, Shun Zhang, Jizhou Song, and Guoliang Huang. Experimental demonstration of a dissipative multi-resonator metamaterial for broadband elastic wave attenuation. *Journal of Sound and Vibration*, 438:1–12, 2019.
- [3] Penglin Gao, Alfonso Climente, José Sánchez-Dehesa, and Linzhi Wu. Single-phase metamaterial plates for broadband vibration suppression at low frequencies. *Journal of Sound and Vibration*, 444:108–126, 2019.
- [4] Yuexia Liu, Wenliang Guo, and Tiancheng Han. Arbitrarily polygonal transient thermal cloaks with natural bulk materials in bilayer configurations. *International Journal of Heat and Mass Transfer*, 115:1–5, 2017.
- [5] Guoqiang Xu, Haochun Zhang, Quan Zou, and Yan Jin. Predicting and analyzing interaction of the thermal cloaking performance through response surface method. *International Journal of Heat and Mass Transfer*, 109:746–754, 2017.
- [6] Guoqiang Xu, Haochun Zhang, Quan Zou, Yan Jin, and Ming Xie. Forecast of thermal harvesting performance under multi-parameter interaction with response surface methodology. *International Journal of Heat and Mass Transfer*, 115:682–693, 2017.
- [7] Garuda Fujii, Youhei Akimoto, and Masayuki Takahashi. Exploring optimal topology of thermal cloaks by CMA-ES. *Applied Physics Letters*, 112(6):061108, 2018.
- [8] Jin Qin, Wei Luo, Peng Yang, Biao Wang, Tao Deng, and Tiancheng Han. Experimental demonstration of irregular thermal carpet cloaks with natural bulk material. *International Journal of Heat and Mass Transfer*, 141:487–490, 2019.

- [9] Guoqiang Xu, Xue Zhou, and Jiayin Zhang. Bilayer thermal harvesters for concentrating temperature distribution. *International Journal of Heat and Mass Transfer*, 142:118434, 2019.
- [10] Garuda Fujii and Youhei Akimoto. Topology-optimized thermal carpet cloak expressed by an immersed-boundary level-set method via a covariance matrix adaptation evolution strategy. *International Journal of Heat and Mass Transfer*, 137:1312–1322, 2019.
- [11] Garuda Fujii and Youhei Akimoto. Cloaking a concentrator in thermal conduction via topology optimization. *International Journal of Heat and Mass Transfer*, 159:120082, 2020.
- [12] Liujun Xu and Jiping Huang. Controlling thermal waves with transformation complex thermotics. *International Journal of Heat and Mass Transfer*, 159:120133, 2020.
- [13] Qingxiang Ji, Xueyan Chen, Jun Liang, Vincent Laude, Sébastien Guenneau, Guodong Fang, and Muamer Kadic. Designing thermal energy harvesting devices with natural materials through optimized microstructures. *International Journal of Heat and Mass Transfer*, 169:120948, 2021.
- [14] Boyan Tian, Jun Wang, Gaole Dai, Xiaoping Ouyang, and Jiping Huang. Thermal metadevices with geometrically anisotropic heterogeneous composites. *International Journal of Heat and Mass Transfer*, 174:121312, 2021.
- [15] Wei Sha, Mi Xiao, Jinhao Zhang, Xuecheng Ren, Zhan Zhu, Yan Zhang, Guoqiang Xu, Huagen Li, Xiliang Liu, Xia Chen, Liang Gao, Cheng-Wei Qiu, and Run Hu. Robustly printable freeform thermal metamaterials. *Nature Communications*, 12(1), 2021.
- [16] Zhan Zhu, Xuecheng Ren, Wei Sha, Mi Xiao, Run Hu, and Xiaobing Luo. Inverse design of rotating metadevice for adaptive thermal cloaking. *International Journal of Heat and Mass Transfer*, 176:121417, 2021.
- [17] Tiancheng Han, Xiuli Yue, Kaihuai Wen, and Junyi Nangong. Monolayer thermal meta-device with switching functions. *International Journal of Heat and Mass Transfer*, 186:122498, 2022.
- [18] Tao Sun, Xinhua Wang, Xuyun Yang, Tao Meng, Renyang He, and Yuexin Wang. Design of thermal cloak and concentrator with interconnected structure. *International Journal of Heat and Mass Transfer*, 187:122568, 2022.
- [19] Ji-Wang Luo, Li Chen, Zihan Wang, and WenQuan Tao. Topology optimization of thermal cloak using the adjoint lattice Boltzmann method and the level-set method. *Applied Thermal Engineering*, 216:119103, 2022.
- [20] Makoto Nakagawa, Yuki Noguchi, Kei Matsushima, and Takayuki Yamada. Level set-based multiscale topology optimization for a thermal cloak design problem using the homogenization method. *International Journal of Heat and Mass Transfer*, 207:123964, 2023.
- [21] Xiaoqiang Xu, Xianfeng David Gu, and Shikui Chen. Topology optimization of thermal cloaks in euclidean spaces and manifolds using an extended level set method. *International Journal of Heat and Mass Transfer*, 202:123720, 2023.
- [22] Juan Manuel Restrepo-Flórez and Martin Maldovan. Mass Separation by Metamaterials. *Scientific Reports*, 6(1), 2016.
- [23] Juan Manuel Restrepo-Flórez and Martin Maldovan. Mass diffusion cloaking and focusing with metamaterials. *Applied Physics Letters*, 111(7):071903, 2017.
- [24] Hao-Chun Zhang, Yi-Yi Li, Zhuang Ma, and Quan Zou. Control Characteristics of Mass Diffusion in a Meta-Material Based on Transformation Coordinate Method. In *ASME 2019 6th International Conference on Micro/Nanoscale Heat and Mass Transfer*. American Society of Mechanical Engineers, jul 2019.
- [25] Yang Li, Chengye Yu, Chuanbao Liu, Zhengjiao Xu, Yan jing Su, Lijie Qiao, Ji Zhou, and Yang Bai. Chemical-diffusion Metamaterials with “Plug and Switch” Modules for Ion Cloaking, Concentrating and Selection: Design and Experiments. *Nature Communications*, 2021.
- [26] Tiemo Bückmann, Michael Thiel, Muamer Kadic, Robert Schittny, and Martin Wegener. An elasto-mechanical unfeability cloak made of pentamode metamaterials. *Nature Communications*, 5(1), 2014.
- [27] Tiemo Bückmann, Muamer Kadic, Robert Schittny, and Martin Wegener. Mechanical cloak design by direct lattice transformation. *Proceedings of the National Academy of Sciences*, 112(16):4930–4934, 2015.
- [28] Víctor D. Fachinotti, Ignacio Peralta, and Alejandro E. Albanesi. Optimization-based design of an elastostatic cloaking device. *Scientific Reports*, 8(1), 2018.
- [29] L. Ai and X.-L. Gao. Three-dimensional metamaterials with a negative Poisson’s ratio and a non-positive coefficient of thermal expansion. *International Journal of Mechanical Sciences*, 135:101–113, 2018.
- [30] Juan C. Álvarez Hostos, Víctor D. Fachinotti, and Ignacio Peralta. Metamaterial for elastostatic cloaking under thermal gradients. *Scientific Reports*, 9(1), 2019.
- [31] Juan C. Álvarez Hostos, Víctor D. Fachinotti, and Ignacio Peralta. Computational design of thermo-mechanical metadevices using topology optimization. *Applied Mathematical Modelling*, 90:758–776, 2021.
- [32] Ulf Leonhardt. Optical conformal mapping. *Science*, 312:1777–1780, 2006.
- [33] John B. Pendry, David Schurig, and David R. Smith. Controlling electromagnetic fields. *Science*, 312(5781):1780–1782, 2006.
- [34] Sebastien Guenneau, Claude Amra, and Denis Veynante. Transformation thermodynamics: cloaking and concentrating heat flux. *Optics Express*, 20(7):8207, 2012.
- [35] Muamer Kadic, Tiemo Bückmann, Robert Schittny, and Martin Wegener. Metamaterials beyond electromagnetism. *Reports on Progress in Physics*, 76(12):126501, 2013.
- [36] Ignacio Peralta, Víctor D. Fachinotti, and Juan C. Álvarez Hostos. A Brief Review on Thermal Metamaterials for Cloaking and Heat Flux Manipulation. *Advanced Engineering Materials*, 22(2):1901034, 2019.

- [37] Juan C. Álvarez Hostos, Víctor D. Fachinotti, Ignacio Peralta, and Benjamín A. Tourn. Computational design of metadevices for heat flux manipulation considering the transient regime. *Numerical Heat Transfer, Part A: Applications*, pages 1–16, 2019.
- [38] Yu-Lin Tsai, Jiangyu Li, and Tungyang Chen. Simultaneous focusing and rotation of a bifunctional thermal metamaterial with constant anisotropic conductivity. *Journal of Applied Physics*, 126(9):095103, 2019.
- [39] Tianzhi Yang, Lujun Huang, Fei Chen, and Weikai Xu. Heat flux and temperature field cloaks for arbitrarily shaped objects. *Journal of Physics D: Applied Physics*, 46(30):305102, 2013.
- [40] Mao Fu-Chun, Li Ting-Hua, Huang Ming, Yang Jing-Jing, and Chen Jun-Chang. Research and design of thermal cloak in arbitrary shape. *Acta Physica Sinica*, 63(1):014401, 2014.
- [41] Tianzhi Yang, Qinghe Wu, Weikai Xu, Di Liu, Lujun Huang, and Fei Chen. A thermal ground cloak. *Physics Letters A*, 380(7-8):965–969, 2016.
- [42] Ignacio Peralta, Víctor D. Fachinotti, and Ángel A. Ciarbonetti. Optimization-based design of a heat flux concentrator. *Scientific Reports*, 7(1), 2017.
- [43] Ignacio Peralta and Víctor D. Fachinotti. Optimization-based design of heat flux manipulation devices with emphasis on fabricability. *Scientific Reports*, 7(6261), 2017.
- [44] Víctor D. Fachinotti, Ángel A. Ciarbonetti, Ignacio Peralta, and Ignacio Rintoul. Optimization-based design of easy-to-make devices for heat flux manipulation. *International Journal of Thermal Sciences*, 128:38–48, 2018.
- [45] Gennady V. Alekseev and Dmitry A. Tereshko. Particle swarm optimization-based algorithms for solving inverse problems of designing thermal cloaking and shielding devices. *International Journal of Heat and Mass Transfer*, 135:1269–1277, jun 2019.
- [46] Garuda Fujii, Hayato Watanabe, Takayuki Yamada, Tsuyoshi Ueta, and Mamoru Mizuno. Level set based topology optimization for optical cloaks. *Applied Physics Letters*, 102(25):251106, 2013.
- [47] S. Narayana, S. Savo, and Y. Sato. Transient heat flux shielding using thermal metamaterials. *Applied Physics Letters*, 102:201904, 2013.
- [48] O. C. Zienkiewics. *The finite element method*. Elsevier/Butterworth-Heinemann, 2005.
- [49] Perumal Nithiarasu, Roland W. Lewis, and Kankanhalli N. Seetharamu. *Fundamentals of the Finite Element Method for Heat and Mass Transfer*. Wiley & Sons, Limited, John, 2016.
- [50] Lucas Colabella, Adrián P. Cisilino, Victor Fachinotti, and Piotr Kowalczyk. Multiscale design of elastic solids with biomimetic cancellous bone cellular microstructures. *Structural and Multidisciplinary Optimization*, 60(2):639–661, 2019.
- [51] Lucas Colabella, Adrián Cisilino, Victor Fachinotti, Carlos Capiel, and Piotr Kowalczyk. Multiscale design of artificial bones with biomimetic elastic microstructures. *Journal of the Mechanical Behavior of Biomedical Materials*, 108:103748, 2020.
- [52] Ercan M. Dede, Tsuyoshi Nomura, and Jaewook Lee. Thermal-composite design optimization for heat flux shielding, focusing, and reversal. *Structural and Multidisciplinary Optimization*, 49(1):59–68, 2013.
- [53] Panagiotis Michaleris, Daniel A. Tortorelli, and Creto A. Vidal. Tangent operators and design sensitivity formulations for transient non-linear coupled problems with applications to elastoplasticity. *International Journal for Numerical Methods in Engineering*, 37(14):2471–2499, 1994.
- [54] Krister Svanberg. The method of moving asymptotes—a new method for structural optimization. *International Journal for Numerical Methods in Engineering*, 24(2):359–373, 1987.
- [55] Martin P. Bendsøe and Ole Sigmund. *Topology optimization. Theory, methods, and applications*. Springer-Verlag, 2003.
- [56] Michele Brun, Sébastien Guenneau, and Alexander B. Movchan. Achieving control of in-plane elastic waves. *Applied Physics Letters*, 94(6):061903, 2009.
- [57] J. K. Guest, J. H. Prévost, and T. Belytschko. Achieving minimum length scale in topology optimization using nodal design variables and projection functions. *International Journal for Numerical Methods in Engineering*, 61(2):238–254, 2004.
- [58] Ole Sigmund. Morphology-based black and white filters for topology optimization. *Structural Multidisciplinary Optimization*, 33:401–424, 2007.
- [59] Erik Andreassen, Anders Clausen, Mattias Schevenels, Boyan S. Lazarov, and Ole Sigmund. Efficient topology optimization in MATLAB using 88 lines of code. *Structural and Multidisciplinary Optimization*, 43(1):1–16, 2010.
- [60] Tyler E. Bruns and Daniel A. Tortorelli. Topology optimization of non-linear elastic structures and compliant mechanisms. *Computer Methods in Applied Mechanics and Engineering*, 190(26-27):3443–3459, 2001.
- [61] Joe Alexandersen, Ole Sigmund, and Niels Aage. Large scale three-dimensional topology optimisation of heat sinks cooled by natural convection. *International Journal of Heat and Mass Transfer*, 100:876–891, 2016.
- [62] Younghwan Joo, Ikjin Lee, and Sung Jin Kim. Topology optimization of heat sinks in natural convection considering the effect of shape-dependent heat transfer coefficient. *International Journal of Heat and Mass Transfer*, 109:123–133, 2017.
- [63] Lei Li and Kapil Khandelwal. Volume preserving projection filters and continuation methods in topology optimization. *Engineering Structures*, 85:144–161, 2015.
- [64] Mattias Schevenels and Ole Sigmund. On the implementation and effectiveness of morphological close-open and open-close filters for topology optimization. *Structural and Multidisciplinary Optimization*, 54(1):15–21, 2016.